Dual Tracer ^{99m}Tc-Pertechnetate / ^{99m}Tc-MIBI Dual-Time-Point SPECT/CT Parathyroid Gland Assessment Regarding to Parathyroid Gland Size and Biochemical Parameters – Two Years Single Imaging Centre Experience

Eva Krčálová[1,2,*], Jiří Horáček[2,3], Edita Nováková[4], Miroslav Cvejn[5], Daša Lazaráková[6], Radek Mikulecký[6], Jiří Máslo[7], Jitka Čepková[8], Jan Tilšer[1], Jiří Doležal[1]

ABSTRACT

Introduction: Preoperative parathyroid imaging is inevitable part of focused parathyroid surgery. The aim of our study was assessment of parathyroid scintigraphy diagnostic accuracy regarding to size and metabolic parameters of hyperfunctioning parathyroid tissue.
Material and methods: Parathyroid scintigraphy for suspected primary hyperparathyroidism was performed in 95 patients during years 2015 and 2016. Of them, 75 patients with known clinical outcome (40 underwent surgery, 35 had documented laboratory follow-up) were further retrospectively evaluated. The performance of dual tracer ^{99m}Tc-pertechnetate and ^{99m}Tc-MIBI subtraction and dual-time-point ^{99m}Tc-MIBI imaging with SPECT/CT was analysed. Serum parathyroid hormone (PTH), calcaemia, ionized calcaemia and phosphataemia and ultrasound detected adenoma volume and largest diameter in false negative and true positive findings were compared using Mann-Whitney test.
Results: Sensitivity and specificity of parathyroid scintigraphy was 74.5% and 95.8%, respectively. NPV was 63.8% and PPV 97.4%. Hyperfunctioning parathyroid tissue detectability was almost significantly associated with hypophosphataemia and PTH levels.
Conclusion: Parathyroid scintigraphy provides high sensitivity and superior specificity in parathyroid adenoma location, nevertheless the diagnostic accuracy tends to decline in smaller adenomas and in less metabolically active parathyroid tissue causing only subtle biochemical changes. ^{18}F-Fluorocholine PET/CT or 3D SPECT/CT subtraction should be a reasonable option for those cases.

KEYWORDS

hyperparathyroidism; primary; single photon emission computed tomography; computed tomography; ultrasonography; parathyroid hormone; hypercalcemia; hypophosphatemia

AUTHOR AFFILIATIONS

[1] Nuclear Medicine Department, University Hospital Hradec Králové, Czech Republic
[2] Academic Department of Internal Medicine, Charles University, Faculty of Medicine in Hradec Králové, Czech Republic
[3] 4th Department of Internal Medicine, Charles University, Faculty of Medicine in Hradec Králové and University Hospital Hradec Králové, Czech Republic
[4] Náchod Hospital Internal Medicine Department, Czech Republic
[5] Private Endocrinology Outpatient Clinic, Náchod, Czech Republic
[6] Pardubice Hospital Internal Medicine Department, Czech Republic
[7] Náchod Hospital Osteology Outpatient Clinic, Czech Republic
[8] Department of Clinical Biochemistry, Faculty of Medicine Hradec Králové and University Hospital Hradec Králové
* Corresponding author: Nuclear Medicine Department, University Hospital Hradec Králové, Sokolská 581, 500 05, Hradec Králové, Czech Republic; e-mail: krcalova.e@gmail.com

Received: 27 November 2018
Accepted: 6 December 2018
Published online: 1 April 2019

Acta Medica (Hradec Králové) 2019; 62(1): 1–5
https://doi.org/10.14712/18059694.2019.38

INTRODUCTION

Primary hyperparathyroidism (pHPT) is a common endocrine disorder, nowadays most frequently disclosed in asymptomatic patients during their routine laboratory check-ups including calcaemia measurements (1, 2). Consequently, the patients are referred to parathyroidectomy during the early disease stage. This trend leads to a shift in surgical approach from bilateral neck exploration to mini-invasive surgery. However, this less invasive approach is suitable only for patients with successfully localized solitary adenoma (3).

Parathyroid scintigraphy plays an essential role in selecting patients for appropriate surgical treatment, allowing precise solitary adenomas location as well as disclosure of supernumerary or ectopic parathyroid glands.

^{99m}Tc labelled lipophilic cation methoxyisobutilisonitrile (^{99m}Tc-MIBI) is used for parathyroid scintigraphy. The tracer is accumulated in tissues with intensive oxidative metabolism (due to its high mitochondrial affinity) including thyroid and parathyroid glands (4). Dual-time-point ^{99m}Tc-MIBI imaging is based on markedly delayed ^{99m}Tc-MIBI wash-out from hyperfunctioning parathyroid tissue (5) (Fig. 1a, b). Scintigraphy spatial resolution is enhanced by single photon emission tomography combined with CT (SPECT/CT) (Fig. 2) and accuracy is improved employing ^{99m}Tc-pertechnetate subtraction (6) (Fig. 3a, b, c). ^{99m}Tc-pertechnetate uptake, limited to the thyroid gland, enables us to distinguish "hot" or "cold" nodules which may interfere with ^{99m}Tc MIBI scan (6).

However, the recent trend to operate patients during the early disease course could potentially lead to decreased sensitivity of preoperative localization procedures, due to lower preoperative serum ionised calcium levels and smaller adenoma size (7).

Thus the aim of our study was to evaluate sensitivity, specificity, positive predictive value (PPV), negative predictive value (NPV) and diagnostic accuracy of our parathyroid imaging protocol. Our secondary aim was to compare serum calcaemia (both total and ionized), phosphataemia, serum parathyroid hormone (PTH) levels and sonographically (US) assessed volume and the longest diameter between true positive and false negative findings.

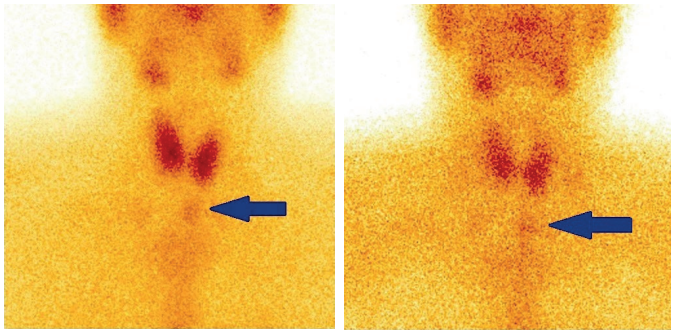

Fig. 1 (a) Early planar scan acquired 10 minutes after ^{99m}Tc-MIBI administration. Arrow shows suspected parathyroid adenoma. (b) Delayed scan obtained 2 hours after ^{99m}Tc-MIBI administration. Arrow shows the same suspected adenoma with markedly delayed radiotracer wash-out.

MATERIALS AND METHODS

We retrospectively reviewed 96 patients with suspected pHPT who underwent parathyroid imaging at the Nuclear Medicine Department of the University Hospital in Hradec Králové from January 2015 till December 2016. Only patients with known clinical outcome (total 75; 40 of them operated and 35 managed conservatively) were further evaluated. In the operated patients, the diagnosis of pHPT was derived from histopathology. In the conservatively managed patients, the diagnosis was assessed from clinical and laboratory follow-up data: ongoing hypercalcaemia and hyperparathyroidism were considered strongly suggestive of pHPT.

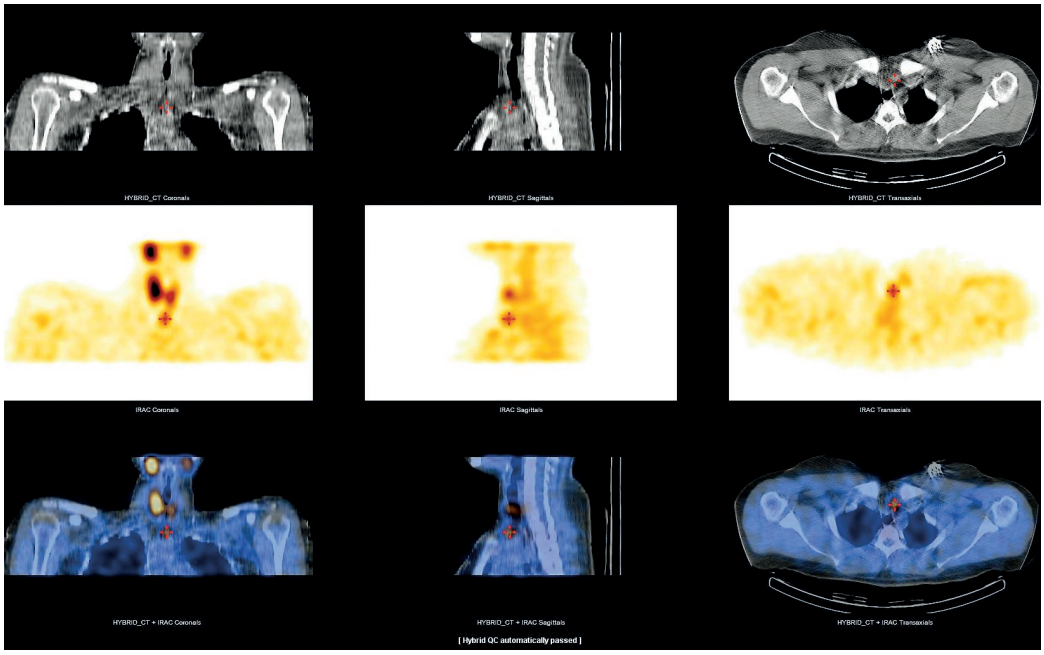

Fig. 2 Neck ^{99m}Tc-MIBI SPECT/CT. Parathyroid adenoma is clearly visible behind the left clavicle.

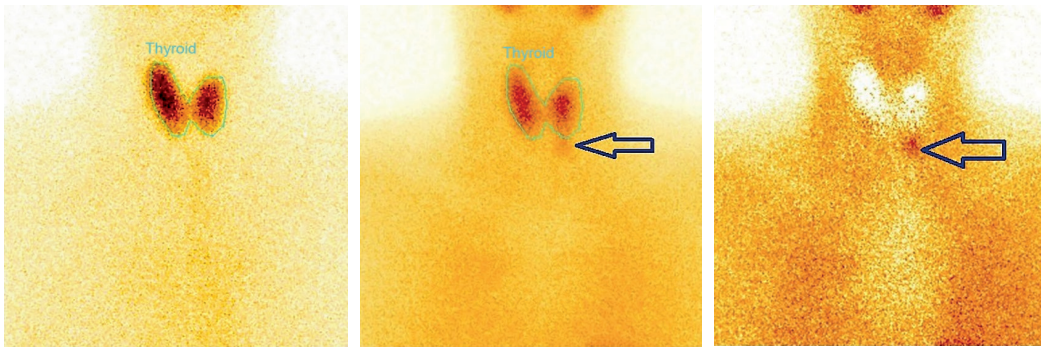

Fig. 3 (a) Planar scan after ^{99m}Tc-pertechnetate administration in another patient. Only thyroid gland is visible. (b) Early planar scan acquired 10 minutes after ^{99m}Tc-MIBI administration, suspected adenoma under the left lobe is faintly visible (arrow). (c) Suspected parathyroid adenoma is clearly depicted using ^{99m}Tc-pertechnetate and ^{99m}Tc-MIBI subtraction (arrow).

Tab. 1 Patients baseline characteristics.

Patients baseline characteristics					
Number of patients, *n*		75			
Gender, *n* (%)	Female	66 (88%)			
	Male	9 (12%)			
Metabolic and ultrasound parameters		**n**	**mean**	**median**	**range**
Calcemia (*mmol/l*)		71	2.73	2.75	2.63–2.86
Serum ionized calcium (*mmol/l*)		53	1.41	1.42	1.29–1.52
Phosphatemia (*mmol/l*)		42	0.84	0.86	0.67–0.97
PTH levels (*pmol/l*)		69	14.69	11.23	8.4–15.7
US lesion largest diameter (*mm*)		45	13.45	12.00	9–15
US lesion volume (*ml*)		30	0.91	0.32	0.21–0.65

Patient characteristics are shown in Table 1. Baseline laboratory parameters and US assessment of suspiciously enlarged parathyroid gland were provided by the referring endocrinologists. 1-84 PTH analyses were performed using chemiluminescence imunoanalysis (system DiaSorin, Stillwater, USA), chemiluminescent microparticle immunoassay (system Architect iSystem, Abbot, Wiesbaden, Germany) and electrochemiluminescence analysis (system Cobas 6000, e601 module Roche diagnostics, Mannheim, DE).

Imaging was performed using a SPECT/CT scanner Infinia Hawkeye 4 (GE Healthcare, Haifa, Israel). Thyroid gland scans (matrix 128 × 128, 500 000 counts) were obtained 20 minutes after 70 MBq ^{99m}Tc-pertechnetate intravenous administration. Subsequently, 700MBq of ^{99m}Tc-MIBI was injected and early planar scan (from upper pole of parotid glands to diaphragm, matrix 128 × 128, 500 000 counts) was acquired 10 minutes thereafter.

Both planar scans were subtracted. This was followed by SPECT/CT acquisition (128 × 128 matrix, 120 projections, 15 seconds per view; low dose CT parameters: 120 kV, 2.5 mAs). Delayed scan (for wash-out assessment) was obtained 2 hours after the early ^{99m}Tc-MIBI scan. The images were evaluated using dedicated software for hybrid imaging (Volumetrix, GE Healthcare). For statistical analysis, SigmaStat software package (Jandel Corporation, San Rafael, CA, USA), version 3.1, was used. As data were mostly non-normally distributed their summary values were expressed as medians (25th–75th percentiles) and comparisons between true positive and false negative findings were performed using non-parametric Mann-Whitney test.

RESULTS

We assessed 75 patients (65 women, 10 men; median age 65 years; range 55–72 years) with suspected pHPT who underwent parathyroid scintigraphy and had reliably documented clinical outcome. Parathyroid scan was true positive in 38 patients, false negative in 13 patients, true negative in 23 patients and false positive in 1 patient as shown in Table 2. The sensitivity of our scintigraphic protocol reached 74.5%, specificity 95.8%, positive predictive value 97.4% but negative predictive value was only 63.8%, as summarized in Table 3.

Tab. 2 Pivot table evaluating parathyroid scintigraphy detection efficiency regarding to clinical outcome (histopatological, imaging or laboratory proof of hyperfunctioning parathyroid tissue).

	Clinical outcome +	**Clinical outcome –**
Scintigraphy +	38	1
Scintigraphy –	13	23

Tab. 3 Patient-based sensitivity, specificity, positive predictive value (PPV), negative predictive value (NPV) and accuracy based on true-positive, true-negative, false-positive and false-negative parathyriod scintigraphy results.

No. of patients	**Sensitivity**	**Specificity**	**PPV**	**NPV**	**Accuracy**
(n)	(%)	(%)	(%)	(%)	(%)
75	74.5	95.8	97.4	63.8	81.3

Tab. 4 Comparison of laboratory parameters and ultrasound findings in parathyroid scan true positive and false negative patients. The p value was calculated using Mann-Whitney test, significance level <0.05.

	Serum PTH (pmol/l)	p	Calcaemia (mmol/l)	p	Ionized calcaemia (mmol/l)	p	Phospha-taemia (mmol/l)	p	Longest diameter (mm)	p	Parathyroid gland volume (ml)	p
True positives	14.05 (10.83;23.47) n = 34	0.088	2.8 (2.69;2.93) n = 34	0.454	1.45 (1.36;1.60) n = 25	0.287	0.66 (0.6;0.78)	0.078	14.0 (11.0;16.0) n = 16	0.233	0.47 (0.30;0.73) n = 14	0.156
False negtives	10.20 (8.75;13.10) n = 11		2.78 (2.65;2.89) n = 13		1.32 (1.17;1.57) n = 11		0.845 (0.68;0.92)		11.0 (10;14) n = 9		0.23 (0.19;0.44) n = 7	

All but one true positive patients underwent neck US and enlarged parathyroid glands were detectable in 26 of 37 of them. Neck US was performed in 12 of 13 false negative patients, and revealed enlarged parathyroid tissue in 9 patients. Baseline neck US performed in 69 of all identified patients (n = 75) reached overall sensitivity 71.4%, specificity only 50.0%, PPV 77.0%, NPV only 41.7% and accuracy 65.0%. Because US is highly operator dependent and neck US examinations were performed by referring endocrinologists, the data inevitably vary in quality.

Although the largest diameter was lower in false negative patients than in true positive ones, the difference did not reach statistical significance. The same was true for parathyroid tissue volume and calcaemia (both total and ionized). The differences in PTH levels and phosphataemia between true positive patients and false negative ones were even more obvious but still slightly above statistical significance level (Table 4).

DISCUSSION

We achieved superior specificity and very high PPV using our dual tracer dual-time-point imaging protocol with SPECT/CT in comparison with the recent study by Raruenrom et al. that report sensitivity 80%, specificity 75%, PPV 88.9%, NPV 60% and accuracy 78.6% using the same comprehensive imaging (8). Neumann et al. who performed ^{123}I-NaI/^{99m}Tc-MIBI subtraction and SPECT/CT achieved higher patient-based 88% sensitivity and the same 96% specificity (9). Nevertheless our NPV and sensitivity were lower than expected.

Despite the similarity of mean longest diameters of our true positive and false negative findings with data published by Behesti et al. (15.5 ± 7.9 mm in our true positives versus 12.2 ± 4.6 mm in false negatives compared to their 17.6 ± 7.4 mm and 13.3 ± 6.7 mm, respectively) and the clearly visible trend of missing smaller adenomas, we (unlike them) failed to prove statistical significance of size differences between true positive and false negative findings (10). This is probably caused by our smaller cohort. This may also apply to parathyroid adenoma volume.

Although small size of parathyroid adenomas (below the gamma camera spatial resolution) is limiting for imaging, accurate location of even subcentimetre parathyroid adenomas is required in the minimal invasive surgery era. On the other hand, high tracer uptake in parathyroid adenomas with intensive metabolism enables detection of such lesions (11). In our analysis, successfully detected parathyroid adenomas volume ranged from 0.3 to 0.7 millilitres and metabolic changes (particularly PTH levels and phosphataemia) were more pronounced in those patients. However, the metabolic changes did not reach statistical significance in our study.

In fact, association between metabolic markers and parathyroid scintigraphy positivity differs from study to study. Formerly published data provided evidence that PTH is significantly higher in parathyroid scan true positive patients (12). Also recent study by Hoang et al. found an association between positive ^{99m}Tc-MIBI scan and higher serum ionised calcium, increased intact PTH levels and lower phosphataemia (13). However, an association between PTH and parathyroid scan positivity was not confirmed by Dy et al. (14). In addition, Behesti et al. recently did not prove statistically significant difference in calcaemia and PTH levels regarding to parathyroid adenomas detectability using ^{99m}Tc-MIBI SPECT/CT (10).

Here, it is necessary to address the issue of normocalcaemic hyperparathyroidism and hypercalcaemia with inappropriately high-normal PTH (normohormonal pHPT). Diagnosis of normocalcaemic hyperparathyroidism can only be established if vitamin D deficiency, chronic kidney disease, malabsorption, idiopathic hypercalciuria and PTH increase due to medication are excluded (1). Normohormonal pHPT is defined as hypercalcaemia without suppressed PTH levels, presuming that other causes of hypercalcaemia like malignancy, granulomatous diseases, vitamin D intoxication, renal disease or thiazides or lithium intake have been ruled out (15). The increasing number of recognized normocalcemic pHPT may explain contradictory data regarding to metabolic differences in true positive and false negative findings in recent studies (16). Because parathyroid surgery is required in all asymptomatic patients younger than 50 years as well as in those with proven subclinical bone or renal impairment (17), localization of such lesions is a big challenge for preoperative parathyroid imaging procedures. A very promising scintigraphic method is 3D subtraction of ^{99m}Tc-pertechnetate and ^{99m}Tc-MIBI SPECT data (18). Nuclear medicine option with superior spatial resolution and sensitivity is ^{18}F-Fluorocholine PET/CT. ^{18}F-Fluorocholine (FCH) is marker of cell membrane turnover (19). Sensitivity of 94%, specificity 96%, PPV 90.2%, NPV 97.4% and diagnostic accuracy 95.3% were achieved using this tracer, making it the most promising tracer with high diagnostic performance (10, 20). At present, PET/CT centres in the

Czech Republic depend on FCH supplies from abroad. This dramatically decreases tracer availability due to its short physical half-life (109 minutes). Marketing authorisation of FCH produced in the Czech Republic for parathyroid imaging is an inevitable step forward to precise preoperative localization of even early and asymptomatic forms of primary hyperparathyroidism.

CONCLUSION

We achieved good sensitivity, superior specificity and PPV using our one day dual tracer dual-time-point imaging protocol with SPECT/CT. Our data suggest that the lower NPV probably results from missing smaller adenomas and hyperfunctioning parathyroid tissue in patients in the early stage of disease. In view of recently published data, ^{18}F-FCH PET/CT or 3D SPECT/CT subtraction may be reasonable options for patients with asymptomatic, normohormonal and normocalcemic pHPT.

ACKNOWLEDGEMENTS

This work was supported by the programme PROGRES Q40-14.

REFERENCES

1. Zajíčková K. Primární hyperparatyreóza - nové klinické formy onemocnění. Vnitř Lék 2017; 63(9): 604–8.
2. Insogna KL. Primary Hyperparathyroidism. N Engl J Med 2018; 379(11): 1050–9.
3. Betka J, Astl J, Chovanec M, Lukeš P, Zábrodský M, Plzák J. Minimálně invazivní endoskopická chirurgie štítné žlázy a příštítných tělísek. Endoskopie 2009; 18(3): 112–5.
4. Mettler FA, Guiberteau MJ. Essentials of nuclear medicine imaging. 6th ed. Philadelphia: Elsevier Saunders, 2012: 126–36.
5. Ziessman HA, O'Malley JP, Thrall JH, Fahey FH. Nuclear medicine: The requisites. Philadelphia: Elsevier Saunders, 2014: 92.
6. Hindié E, Ugur Ö, Fuster D, et al. 2009 EANM parathyroid guidelines. Eur J Nucl Med Mol Imaging 2009; 36(7): 1201–16.
7. Almquist M, Bergenfelz A, Mårtensson H, Thier M, Nordenström E. Changing biochemical presentation of primary hyperparathyroidism. Langenbecks Arch Surg 2010; 395(7): 925–8.
8. Raruenrom Y, Theerakulpisut D, Wongsurawat N, Somboonporn C. Diagnostic accuracy of planar, SPECT, and SPECT/CT parathyroid scintigraphy protocols in patients with hyperparathyroidism. Nucl Med Rev Cent East Eur 2018; 21(1): 20–5.
9. Neumann DR, Obuchowski NA, DiFilippo FP. Preoperative ^{123}I/^{99m}Tc-Sestamibi Subtraction SPECT and SPECT/CT in Primary Hyperparathyroidism. J Nucl Med 2008; 49: 2012–7.
10. Beheshti M, Hehenwarter L, Paymani Z, et al. ^{18}F-Fluorocholine PET/CT in the assessment of primary hyperparathyroidism compared with ^{99m}Tc-MIBI or ^{99m}Tc-tetrofosmin SPECT/CT: a prospective dual-centre study in 100 patients. Eur J Nucl Med Mol Imaging 2018; 45(10): 1762–71.
11. Koranda P, Halenka M, Zahálková J, Kosatíková Z , Mysliveček M. Jednodenní scintigrafické vyšetření kombinující ^{99m}Tc MIBI/ ^{99m}TcO4 subtrakci a dvoufázvou ^{99m}Tc-MIBI scintigrafii a SPECT u pacientů s terciární hyperparatyreózou. Ces Radiol 2010; 64(3): 192–7.
12. Westerdahl J, Bergenfelz A. Sestamibi scan-directed parathyroid surgery: potentially high failure rate without measurement of intraoperative parathyroid hormone. World J Surg 2004; 28(11): 1132–8.
13. Hoang TD, Jani AG, Mai VQ, Tuamokumo FO, Shakir MKM. Associations of serum ionized calcium, phosphate and PTH levels with technetium-99 sestamibi parathyroid SPECT/CT scan in primary hyperparathyroidism. Endocr Pract 2019; 25(1): 16–22.
14. Dy BM, Richards ML, Vazquez BJ, Thompson GB, Farley DR, Grant CS. Primary hyperparathyroidism and negative Tc99 sestamibi imaging: to operate or not? Ann Surg Oncol 2012; 19(7): 2272–8.
15. Broulík P. Hyperkalcemie: na co je třeba myslet a jaká vyšetření provést? Interní Med 2011; 13(7–8): 314–7.
16. Silverberg SJ, Clarke BL, Peacock M, et al. Current issues in the presentation of asymptomatic primary hyperparathyroidism: proceedings of the Fourth International Workshop. J Clin Endocrinol Metab 2014; 99(10): 3580–94.
17. Udelsman R, Akerstrom G, Biagini C, et al. The surgical management of asymptomatic primary hyperparathyroidism: proceedings of the Fourth International Workshop. J Clin Endocrinol Metab 2014; 99(10): 3595–606.
18. Chroustova D, Kubinyi J, Trnka J, Adamek S. The role of 99mTc-MIBI SPECT/low dose CT with 3D subtraction in patients with secondary hyperparathyroidism due to chronic kidney disease. Endocr Regul 2014; 48(2): 55–63.
19. Huber GF, Hullner M, Schmid C, et al. Benefit of (18)F-fluorocholine PET imaging in parathyroid surgery. Eur Radiol 2018; 28(6): 2700–7.
20. Kluijfhout WP, Pasternak JD, Drake FT, et al. Use of PET tracers for parathyroid localization: a systematic review and meta-analysis. Langenbecks Arch Surg 2016; 401(7): 925–35.

Prevalence of Musculoskeletal Disorders Symptoms among Czech Dental Students. Part 2: the Predictive Value of Digital Assessment

Martin Kapitán[1,*], Nela Pilbauerová[1], Lenka Vavřičková[1], Zdeňka Šustová[1], Stanislav Machač[2,3]

ABSTRACT

This article is the second part of an evaluation of musculoskeletal disorders (MSDs) prevalence among dental students. As the majority of complaints are in the back region, there is an endeavor to analyze objectively the disorders in this region. One of the non-invasive and non-radiation methods is the spinal curve mapping using the Spinal Mouse® device (Idiag AG, Fehraltorf, Switzerland). The aim of this study was to determine a correlation between subjectively described complaints and the results of an objective examination of the spine using the Spinal Mouse® device. Information about the participants is given in the first part of the article. All the participants were examined with the Spinal Mouse® device in several body positions. Further, the Matthiass test was performed to evaluate neuromuscular stabilization of the axial skeleton in static conditions. Musculoskeletal pain occurred more often in students who had a higher range of motion (ROM) and had worse static stabilization of spine. Other assessed factors or measured parameters did not have any influence on musculoskeletal pain. Some of the parameters measured with the Spinal Mouse® device showed a correlation with the prevalence of musculoskeletal pain.

KEYWORDS

dentistry students; musculoskeletal disorders; objective evaluation

AUTHOR AFFILIATIONS

[1] Department of Dentistry, Charles University, Faculty of Medicine in Hradec Králové, and University Hospital Hradec Králové, Hradec Králové, Czech Republic
[2] Institute of Sports Medicine, Prague, Czech Republic
[3] Department of Rehabilitation and Sports Medicine, Charles University, 2nd Faculty of Medicine, and Motol University Hospital, Prague, Czech Republic
* Corresponding author: Department of Dentistry, University Hospital Hradec Králové, Sokolská 581, 500 05, Hradec Králové, Czech Republic; e-mail: kapitanm@lfhk.cuni.cz

Received: 5 August 2018
Accepted: 29 November 2018
Published online: 1 April 2019

Acta Medica (Hradec Králové) 2019; 62(1): 6–11
https://doi.org/10.14712/18059694.2019.39

INTRODUCTION

This article is the second part of an evaluation of musculoskeletal disorders (MSDs) prevalence among dental students.

MSDs occur frequently among dentists (1–6) and they often start already during dentistry studies (7–11). The most frequent areas of pain are neck, lower back and shoulders. As the majority of complaints are in the back region, there is an endeavor to analyze objectively the disorders in this region. If X-ray methods were to be used, they would present a radiation dose for the examined persons and for this reason they are not suitable for screening of asymptomatic individuals (12–14). One of the non-invasive and non-radiation methods available is the spinal curve mapping using the Spinal Mouse® device (Idiag AG, Fehraltorf, Switzerland).

The device is provided with a measuring head with two wheels that automatically adjust themselves to the contour of the spine. During the measuring, the examiner stands behind the examined person and fluently guides the wheels in contact with the skin along the spine over the spinous processes from C7 *processus spinosus* to the beginning of the gluteal groove, where is the presumed position of S3 (Fig. 1). The turning of the wheels and the changes of inclination of the device towards the vertical line are simultaneously recorded during the examination. This data is wirelessly transferred to the computer, where the spinal curve is reconstructed. The device can be used for spinal curve mapping and for an evaluation of the range of motion (ROM) in sagittal and frontal planes (14). The acquired information includes the shape of the spine, the length of measured segments, intersegmental angles, the angles of thoracic kyphosis and lumbar lordosis, the range of motion of the whole spine and in individual segments (Th1/2-L5/S1) and the inclination of the sacrum (12–14). The results are presented in pictures and tables, an example is shown in Figure 2.

Fig. 1 The Spinal Mouse® device.

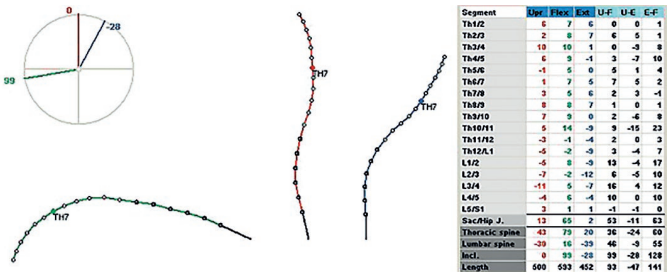

Segment	Upr.	Flex.	Ext.	U-F	U-E	E-F
Th1/2	6	7	6	0	0	1
Th2/3	2	8	7	6	5	1
Th3/4	10	10	1	0	-3	8
Th4/5	6	9	-1	3	-7	10
Th5/6	-1	5	0	5	1	4
Th6/7	1	7	-5	7	5	2
Th7/8	3	5	6	2	3	-1
Th8/9	8	8	7	1	0	1
Th9/10	7	9	0	2	-6	8
Th10/11	5	14	-9	9	-15	23
Th11/12	-3	-1	-4	2	0	3
Th12/L1	-5	-2	-9	3	-4	7
L1/2	-5	8	-9	13	-4	17
L2/3	-7	-2	-12	6	-5	10
L3/4	-11	5	-7	16	4	12
L4/5	-4	6	-4	10	0	10
L5/S1	3	1	1	-1	-1	0
Sac/Hip J.	13	65	2	53	-11	63
Thoracic spine	43	79	20	36	-24	60
Lumbar spine	-39	16	-39	46	-3	55
Incl.	0	99	-28	99	-29	128
Length	500	593	452	93	-47	141

Fig. 2 Example of results of examination. The reconstructed spinal curves in standing upright position, maximal flexion and maximal extension along with the data chart with intervertebral and segmental angles in different body positions.

The relationship between the spinal curve and the development of MSD is not clear. The most common spinal disorders are co-morbid with general health conditions, but there is a lack of clarity in the literature differentiating which conditions are merely co-morbid versus ones that are risk factors (15). It seems that postural defects in the sagittal plane may predict the prevalence of pain with a higher prevalence of pain in people with a higher angle of lumbar lordosis (16). In terms of scoliosis, most findings argue against a major etiological role of the idiopathic scoliotic deformity of adolescents on back pain. However, the impact of pain in adults' scoliosis may be entirely different (17).

Another possible use of this device is an examination of muscular stabilization of the spine, provided by the standardized Matthiass test. This test is one of the methods for objectification of the neuromuscular stabilization of the axial skeleton in static conditions. Impaired neuromuscular stabilization is considered to be an important factor in the development of MSDs. Functioning interplay between the diaphragm, pelvic floor, abdominal muscles and paravertebral muscles is crucial for the spinal stabilization (18). Less activation of the transversus abdominis and multifidus muscle in subjects with low back pain may contribute to decrease the lumbar stabilization especially during stoop lift (19). Matthias test was proposed as a diagnostic tool for posture faults measurement. The typical indicator of a weak posture during this test is a forward hip movement accompanied with lumbar extension (20). Such adjustment of static stance means a failure of a dynamic neuromuscular trunk stabilization principle when the diaphragm should hold the position just above the pelvic floor with an appropriate activation together with abdominal muscles (18).

Spinal mouse was proven to be a suitable tool for research and patient follow-up in the clinical setting as a

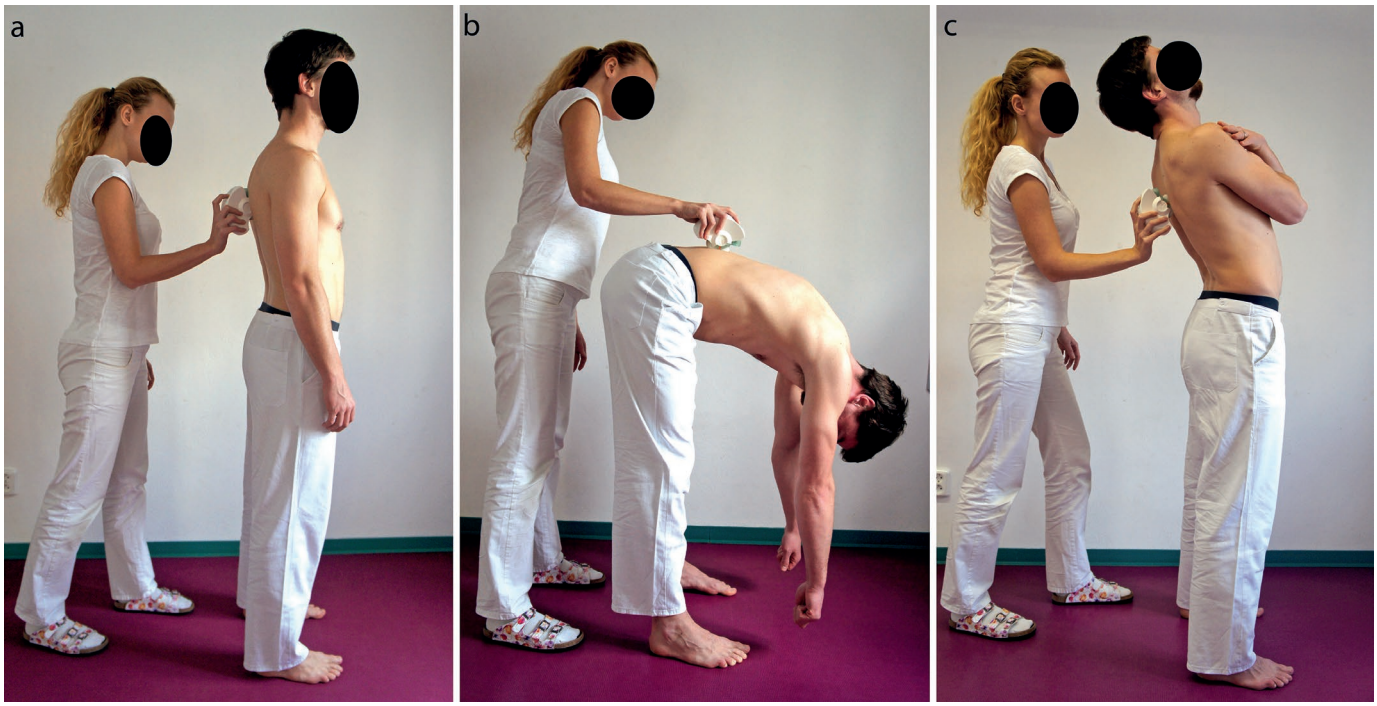

Fig. 3 An examination with the Spinal Mouse® device in standing upright position (a), in maximal flexion (b) and in maximal extension (c).

safe, reliable, quick, and easy to use method with no side effects (21). The reliability was shown to be strong (12). "Armvorhaltetest" according to Matthiass, i.e. so called Matthiass test measures the spinal alignment deviation during upper arms static loading in 90° shoulder flexion (20). This function is included as a standard part of Spinal Mouse® software provided by the manufacturer.

The aim of this study was to gather and analyze information about the prevalence of symptoms of MSDs and the role of potential risk factors among dental students; this is described in the first part of this article. The second aim was to determine a correlation between subjectively described complaints and the results of an objective examination of the spine using the Spinal Mouse® device. The results could contribute to understand the early development of MSDs among dental students and to find out possible risk factors detectable during the objective examination.

MATERIAL AND METHODS

Information about the participants was acquired using a questionnaire and is given in the first part of this article.

All the participants signed an informed consent. This study was approved by the Ethics committee of University Hospital Hradec Králové (Ref. no. 201410 S04P) and by the dean of the Charles University, Faculty of Medicine in Hradec Králové.

All the participants were examined with the Spinal Mouse® device in the sagittal plane. During the examination the participants were measured in three basic positions: standing upright position, maximal flexion and maximal extension; all the positions without knee flexion (Fig. 3a-c). Further, the Matthiass test was performed. During this test the participants held the weight of 1.5 kg in each hand with arms stretched forward. The spinal curve measurement was done in this position at the beginning and was repeated after 30 seconds of staying in this position. The change of the whole spinal inclination (inclination of the

Fig. 4 Matthiass test.

line connecting Th1 and S1 from the vertical line) between the measurements was evaluated (Fig. 4).

The parameters chosen for the statistical analysis of the relationship between the subjectively declared musculoskeletal pain and the results of an objective examination with the Spinal Mouse® device were as follow: thoracic kyphosis angle, lumbar lordosis angle, inclination of the sacrum, the total range of motion, the ratio between the angles of the thoracic kyphosis and the lumbar lordosis (Th/L ratio), and the change of the spine inclination during the Matthiass test.

The collected data were statistically analyzed in the NCSS 10 Statistical Software (2015; NCSS, LLC. Kaysville, Utah, USA, ncss.com/software/ncss) using methods of descriptive statistics, two-sample t-test, nonparametric Mann-Whitney test, Kolmogorov-Smirnov test and nonparametric Kruskal-Wallis analysis of variance with post hoc Dunn's test with Bonferroni modification. The level of statistical significance was set to $\alpha = 0.05$.

RESULTS

A total of 182 students participated in this study; there was a response rate of 94.8%. Their characteristics and answers to the questionnaire are presented in the first part of this article.

The results of the followed parameters measured with the Spinal Mouse® device in total and a comparison between men and women and between the groups of students are summarized in Table 1. As the data were not distributed normally, the median values along with the first and the third quartiles are presented. ROM was statistically significantly higher in the fifth year students than in both the first and the third year students ($p < 0.001$). The difference between the first and the third year students was not statistically significant. There was no statistically significant difference between the years in all other measured parameters.

Musculoskeletal pain was more frequent in students with bigger ROM ($p < 0.05$) and with worse static stabilization of spine evaluated by the Matthiass test ($p < 0.05$). Students with worse static spinal stabilization declared pain in the neck region more often ($p < 0.05$). Other parameters measured with the Spinal Mouse® device didn't have any influence on the prevalence of musculoskeletal pain.

DISCUSSION

The authors endeavored to extend the information from the questionnaires by the data acquired from the objective examination of the participants. The examination with the Spinal Mouse® device is simple, fast and non-invasive and doesn't present any radiation dose for the examined person (13, 14, 22). The measurement is sufficiently valid and reliable in evaluation of longer segments of the spine (12–14, 22–25). During the examination with the Spinal Mouse® device the author encountered several issues. The measurement was difficult in certain participants, mainly women, where there was a sharp angle in the lumbar area during their maximal extension. This was problematic to record because of the size of the device and/or slipping of the wheels (8, 14). The measuring was also difficult in obese individuals for a thicker layer of soft tissues covering the spine (22). An evaluation of individual intervertebral angles may not be valid (26), because the device doesn't measure the angles between the vertebral bodies, but between the spinous processes. Thus, the result may be distorted by the variable angle of spinous processes in individual vertebrae (12). Therefore, the above listed parameters were selected from the Spinal Mouse® measurement results for the statistical analysis. The authors presumed, that a pathology found in the selected parameters may correlate with pain in corresponding regions.

Although the Matthiass test was designed for youngsters between 6 and 16 years, the authors believe that it is

Tab. 1 The results of the Spinal Mouse® examination.

	Total	Gender		Year		
		Male	Female	First	Third	Fifth
	Median (Q1; Q3)	Median (Q1; Q3)	Median (Q1; Q3)	Median (Q1; Q3)	Median (Q1; Q3)	Median (Q1; Q3)
Thoracic kyphosis [°]	35.5 (30; 41)	38 (34; 44)*	34 (30; 39)*	35 (31; 40)	36 (27.5; 41.5)	35.5 (30.25; 42)
Lumbar lordosis [°]	-31 (-37; -24)	-25 (-30; -21)**	-35 (-39; -28)**	-33 (-38; -25)	-32 (-37.5; -24.5)	-30 (-37; -23)
Angulation of the sacrum [°]	19 (14; 24)	14 (10; 17)**	22 (17; 26)**	19 (14; 25)	20 (14; 24)	18.5 (13; 23)
ROM [°]	139 (124; 157)	138 (127; 154)	140 (124; 160)	133 (117.5; 145)	137 (121.5; 151)	151.5 (138.25; 163)**
Th/L ratio	1.15 (0.9; 1.5)	1.5 (1.3; 1.8)**	1 (0.8; 1.2)**	1.1 (0.9; 1.5)	1.2 (0.8; 1.55)	1.2 (0.9; 1.475)
Deviation of Th/L ratio from the value 1	0.3 (0.1; 0.525)	0.5 (0.3; 0.8)**	0.2 (0.1; 0.3)**	0.2 (0.1; 0.55)	0.3 (0.2; 0.55)	0.3 (0.125; 0.575)
Matthiass test [°]	-2 (-3; 0)	-2 (-4; 0)	-2 (-3; 0)	-2 (-3.5; -1)	-2 (-4; 1)	-1 (-3; 0)

* $p < 0.01$; ** $p < 0.001$

applicable also in the young adults and was useful for the purpose of this study, because in contrast with a plain static measurement of the spinal curve shape, it brings the possibility of objectification of neuromuscular stabilization, i.e. an evaluation of the key function of the spine musculature related to the development of the vertebrogenic algic syndrome.

Tsuonda et al. (27) found an influence of lumbar lordosis angle on the cervical spine pain and shoulder pain in a group of 329 volunteers with an average age of 65.5 years. The authors of this study showed in their previous study among dental practitioners with an average age of 38.9 years an influence on the prevalence of musculoskeletal pain by the lumbar lordosis angle, angulation of the sacrum and Th/L ratio (8). On the contrary, the only parameters measured with the Spinal Mouse® with influence on musculoskeletal pain prevalence in this study were ROM and the Matthiass test. An interesting finding was that the worse results in the Matthiass test correlated with higher prevalence of pain in the cervical spine. This shows a close correlation between the neuromuscular stabilization of the thoracic and lumbar spine and the function of the cervical spine. None of the statically measured parameters of the spinal curve shape showed an influence on musculoskeletal pain. The reason may be the relatively low age of the students, where the MSDs are rather of a functional nature and it is not possible to reveal them with statically performed imaging methods. It is also necessary to mention the fact, that the subjectively declared pain is not directly dependent on the structural findings, even in case of advanced imaging methods, such as MRI (28). This can be explained especially by the factor of dynamic neuromuscular stabilization, which is not directly reflected in plain static examination (18). However, the authors assume that the level of neuromuscular trunk stabilization was evaluated by the Matthiass test to a great extent. After several years of dental practice and with an absence of prevention or treatment it can be supposed that MSDs progress more often to structural findings detectable by the Spinal Mouse® device.

A limitation of this study was that different students were involved in different years. For more precise evaluation of the development of the relationship between the musculoskeletal pain and the objective findings it would be useful to evaluate the same students gradually in the first, third and fifth year, followed by an evaluation of the same participants after a few years of dental practice. Also, some other device or method might be used to the objective examination of the locomotive apparatus.

CONCLUSIONS

The correlation of the spinal curve shape in different body positions measured statically in the sagittal plane with the prevalence of musculoskeletal pain was not proved in this study.

The worse neuromuscular stabilization of the spine evaluated by the Matthiass test and the higher ROM of the spine showed a relation with the prevalence of musculoskeletal pain. This indicates that poor neuromuscular spine stability is a risk factor for the development of musculoskeletal pain.

There was a bigger ROM among the fifth year students. No other measured parameter differed between the students in different years.

ACKNOWLEDGEMENTS

The authors declare that they have no competing interests. The authors declare that they are not associated in any way with the producer or distributor of the Spinal Mouse® device, and that the study was not supported by these companies.

The study was financially supported by the Charles University's programme PROGRES Q40/13.

The authors would like to thank Dr. Eva Čermáková from Computer Technology Center, Charles University in Prague, Faculty of Medicine in Hradec Králové, Czech Republic, for help with the statistical analysis, and Ms. Eva Vedralová, Ms. Sara Rezazadeh Siaghi and Ms. Eliska Charlotte Wurfel for a language revision of the manuscript.

REFERENCES

1. European agency for safety and health at work. OSH in figures: Work-related musculoskeletal disorders in the EU-Facts and figures. Luxembourg: Publications Office of the European Union; 2010.
2. Abbas SB, Qazi SR, Iftikhar S, Iqbal MU. Musculoskeletal disorders among dentists and dental students. Pakistan Oral & Dental Journal 2015; 35: 461–5.
3. Abduljabbar TA. Musculoskeletal disorders among dentists in Saudi Arabia. Pakistan Oral & Dental Journal 2008; 28: 135–44.
4. Alexopoulos EC, Stathi IC, Charizani F. Prevalence of musculoskeletal disorders in dentists. BMC Musculoskelet Disord 2004; 9: 16.
5. Hayes MJ, Cockrell D, Smith DR. A systematic review of musculoskeletal disorders among dental professionals. Int J Dent Hyg 2009; 7: 159–65.
6. Hodacova L, Sustova Z, Cermakova E, Kapitan M, Smejkalova J. Self-reported Risk Factors Related to the Most Frequent Musculoskeletal Complaints among Czech Dentists. Ind Health 2015; 53: 48–55.
7. Leggat PA, Smith DR. Musculoskeletal disorders self-reported by dentists in Queensland, Australia. Aust Dent J 2006; 51: 324–7.
8. Pilbauerová N, Kapitán M, Šustová Z, Machač S. An evaluation of the occurrence of musculoskeletal disorders among dentists of the Department of Dentistry, Charles University, Faculty of Medicine in Hradec Králové, and University Hospital Hradec Králové – a pilot study. LKS 2017; 27: 8–12. [in Czech]
9. Puriene A, Aleksejuniene J, Petrauskiene J, Balciuniene I., Janulyte V. Self-reported occupation health issues among Lithuanian dentists. Ind Health 2008; 46: 369–74.
10. Šustová Z, Hodačová L, Kapitán M. The prevalence of musculoskeletal disorders among dentists in the Czech Republic. Acta Medica (Hradec Kralove) 2013; 56: 150–6.
11. Harutunian K, Gargallo-Albiol J, Figueiredo R, Gay-Escoda C. Ergonomics and musculoskeletal pain among postgraduate students and faculty members of the School of Dentistry of the University of Barcelona (Spain). A cross-sectional study. Med Oral Patol Oral Cir Bucal 2011; 16: e425–9.
12. Barrett E, McCreesh K, Lewis J. Reliability and validity of non-radiographic methods of thoracic kyphosis measurement: A systematic review. Manual Therapy 2014; 19: 10–7.
13. Mannion AF, Knecht K, Balaban G, Dvorak J, Grob D. A new skin-surface device for measuring the curvature and global and segmental ranges of motion of the spine: reliability of measurements and comparison with data reviewed from the literature. Eur Spine J 2004; 13: 122–36.
14. Post RB, Leferink VJ. Spinal mobility: sagittal range of motion measured with the Spinal Mouse, a new non-invasive device. Arch Orthop Trauma Surg 2004; 124: 187–92.

15. Green BN, Johnson CD, Haldeman S, et al. A scoping review of biopsychosocial risk factors and co-morbidities for common spinal disorders. PloS One 2018;13(6): e0197987.
16. Zwierzchowska A, Tuz J. Evaluation of the impact of sagittal spinal curvatures on musculoskeletal disorders in young people. Med Pr 2018; 69(1): 29–36. [in Polish]
17. Balague F, Pellise F. Adolescent idiopathic scoliosis and back pain. Scoliosis Spinal Disord 2016; 11(1): 27.
18. Frank C, Kobesova A, Kolar P. Dynamic neuromuscular stabilization & sports rehabilitation Int J Sports Phys Ther 2013; 8: 62–73.
19. Yang HS. Difference of the thickness and activation of trunk muscles during static stoop lift at different loads between subjects with and without low back pain. J Back Musculoskelet Rehabil 2018; 31(3): 481–8.
20. Klee A. Predictive value of Matthiass' arm-raising test. Z Orthop Ihre Grenzgeb 1995; 133(3): 207–13. [in German]
21. Livanelioglu A, Kaya F, Nabiyev V, Demirkiran G, Fırat T. The validity and reliability of "Spinal Mouse" assessment of spinal curvatures in the frontal plane in pediatric adolescent idiopathic thoraco-lumbar curves. Eur Spine J 2016; 25: 476–82.
22. Imagama S, Matsuyama Y, Hasegawa Y, et al. Back muscle strength and spinal mobility are predictors of quality of life in middle-aged and elderly males. Eur Spine J 2011; 20: 954–61.
23. Guermazi M, Ghroubi S, Kassis M, et al. Validity and reability of Spinal Mouse to assess lumbar flexion. Ann Readapt Phy 2006; 49: 172–7. [in French]
24. Kellis E, Adamou G, Tzilios G, Emmanouilidou M. Reliability of spinal range of motion in healthy boys using a skin-surface device. J Manipulative Physiol Ther 2008; 31: 570–6.
25. Topalidou A, Tzagarakis G, Souvatzis X, Kontakis G, Katonis P. Evaluation of the reliability of a new non-invasive method for assessing the functionality and mobility of the spine. Acta Bioeng Biomech 2014; 16: 117–24.
26. Ripani M, Di Cesare A, Giombini A, Agnello L, Fagnani F, Pigozzi F. Spinal curvature: comparison of frontal measurements with the Spinal Mouse and radiographic assessment. J Sports Med Phys Fitness 2008; 48: 488–94.
27. Tsunoda D, Iizuka Y, Iizuka H, et al. Associations between neck and shoulder pain (called katakori in Japanese) and sagittal spinal alignment parameters among the general population. J Orthop Sci 2013; 18: 216–9.
28. Brinjikji W, Luetmer PH, Comstock B, et al. Systematic literature review of imaging features of spinal degeneration in asymptomatic populations. AJNR Am J Neuroradiol 2015; 36: 811–6.

Alteration of Thiol-Disulfide Homeostasis in Fibromyalgia Syndrome

Ayca Tuzcu[1], Rabia Aydogan Baykara[2], Murat Alışık[3], Ahmet Omma[4], Gunseli Karaca Acet[2], Erdal Dogan[2], Medine Cumhur Cure[5], Fatih Duygun[6], Erkan Cure[7,*], Ozcan Erel[8]

ABSTRACT

Background: Fibromyalgia syndrome (FMS) is an extra-articular rheumatological disease, characterized by widespread pain and somatic symptoms. The etiology has not yet been clarified. Oxidative stress may play an important role in FMS etiology. Thiol group is a very strong antioxidant. We aimed to investigate whether thiol/disulfide homeostasis in FMS is altered or not.

Material and methods: A total of 80 female FMS patients and 64 healthy female control individuals were included in this study. Thiol and disulfide values were measured by Erel's novel methods.

Results: Native thiol (330.6 ± 46.1 vs. 356.8 ± 55.5 µmol/L, p = 0.005) and native thiol/total thiol (89.4 ± 3.2 vs. 93.3 ± 4.0, p < 0.001) levels of FMS patients were significantly lower when compared to the values of control group. However, disulfide (19.4 ± 6.3 vs. 12.2 ± 6.3 µmol/L, p < 0.001) levels of FMS patients were significantly higher than healthy individuals. A negative correlation was found between the native thiol/total thiol and fibromyalgia impact questionnaire (FIQ) score among the FMS patients. A positive correlation was found between disulfide values and FIQ score among the patients.

Conclusions: In FMS patients, there was a significant correlation between the decrease in the thiol levels and an increase in the disulfide levels with the FIQ scores. We determined that thiol-disulfide rate was deteriorated in FMS patients and it increases in favor of disulfide amounts.

KEYWORDS

fibromyalgia; thiol; disulfide; thiol/disulfide homeostasis; oxidative stress

AUTHOR AFFILIATIONS

[1] Department of Biochemistry, Malatya Education and Research Hospital, Malatya, Turkey
[2] Department of Physical Medicine and Rehabilitation, Malatya Education and Research Hospital, Malatya, Turkey
[3] Department of Clinical Biochemistry, Ankara Education and Research Hospital, Ankara, Turkey
[4] Division of Rheumatology, Department of Internal Medicine, Numune Education and Research Hospital, Ankara, Turkey
[5] Department of Biochemistry, Istanbul Laboratory, Istanbul, Turkey
[6] Departments of Orthopedics and Traumatology, Antalya Training and Research Hospital, Antalya, Turkey
[7] Department of Internal Medicine, Camlica Erdem Hastanesi, Istanbul, Turkey
[8] Department of Clinical Biochemistry, Faculty of Medicine, Yildirim Beyazit University, Ankara, Turkey
* Corresponding author: Department of Internal Medicine, Camlica Erdem Hastanesi, Uskudar, 34692 Istanbul, Turkey; e-mail: erkancure@yahoo.com

Received: 22 March 2018
Accepted: 12 November 2018
Published online: 1 April 2019

Acta Medica (Hradec Králové) 2019; 62(1): 12–18
https://doi.org/10.14712/18059694.2019.40

INTRODUCTION

Fibromyalgia syndrome (FMS) is an extra-articular rheumatological disease characterized by widespread pain and somatic symptoms. The etiology has not yet been clarified. It is manifested with fatigue, sleep disorders, migraine, depression, irritable bowel disease, panic disorder and decreased pain threshold (1). FMS is generally seen in the middle-aged female populations (2). Although the patients frequently experience musculoskeletal pain, the laboratory findings and the radiological examinations are normal (3). There are various studies reporting the role of genetic and biochemical markers and antibodies in the FMS pathogenesis. Polymorphisms of *5-hydroxytryptamine receptor 2A* (*5-HT2A*), *catechol-O-methyl transferase* (*COMT*) gene, *serotonin transporter* (*SERT*) gene, *substance P* gene, and *cytokines* genes (*Interleukin [IL]-1* and *IL-4*) are defined in FMS. All these gene polymorphisms detected in FMS are associated with monoamine metabolism and transportation. Thus, the products of these genes are severely affected by stress (4–6).

FMS has recently been associated with the deterioration of the oxidative stress and the antioxidant balance. According to the studies, it has been observed that total antioxidant capacity and compounds of the antioxidant defense system are lower in FMS patients when compared to healthy individuals (7). It has also been reported that lipid peroxidation and the oxidative stress increase in FMS. Reactive oxygen specimens (ROS) production is considerably higher in FMS patients as a result of the oxidative stress compared to controls. Increased ROS and decreased coenzyme Q10 levels in FMS are the indicators of mitochondrial dysfunction (8, 9).

Thiols may react with free radicals in order to preserve the organism against tissue and cell injury which can occur due to ROS. Thiols are the compounds that contain sulfhydryl (SH) groups (10). The highest thiol amount in blood plasma exists in albumin and others proteins (11). Thiol groups form disulfide bonds as a result of being reduced by oxidant molecules (12). These structures can turn into thiols again. When the thiol and thiol/disulfide balance is deteriorated, ROS deteriorate the protein structures and cause cellular and tissue damage (13). Erel et al. developed an automated method which can separately measure thiol/disulfide group and the evaluated thiol/disulfide rates significantly change in various diseases (10–14).

In this study, the relationship between the thiol/disulfide balance and the FMS was examined. Furthermore, we also controlled whether or not the thiol/disulfide balance is deteriorated in FMS patients when compared to healthy controls.

METHODS

This cross-sectional study was conducted in our Rheumatology, Physical Medicine and Rehabilitation clinics between January 2016 and April 2016. Eighty female patients who had complaints at least for the last three months and 64 healthy female controls were included in the study. The control group was selected among the voluntary individuals. Patient and control groups were compatible interns of age and body mass index (BMI). Patients were selected according to the ACR 2010 diagnosis criteria (15). Disease activities of FMS patients were evaluated by using Fibromyalgia Impact Questionnaire (FIQ) scores and the sleep quality of patients was assessed by using the Pittsburg sleep quality scale (PSQS). Patients and controls with concomitant systemic situations and additional properties such as vegetarian or vegan, smoking, alcohol use, pregnancy, and breastfeeding were excluded from the study. Furthermore, patients with comorbidities such as hypertension, cardiovascular disease, acute or chronic kidney disease, infections, chronic obstructive pulmonary disease, and malignancies were not included in the study. In addition, individuals who were on any type of medication (including contraceptives) or antioxidants were not included in the control group. Patients who were on drugs other than the ones used for the FMS treatment were not included in the patient group. All of the individuals were informed about the study and their written consents were obtained. The local ethics committee approval was obtained for the study.

FIBROMYALGIA IMPACT QUESTIONNAIRE

FIQ was developed by Burckhard et al. in order to evaluate the functional status of the FMS. The Turkish reliability and validity study of the scale was conducted by Sarmer et al. The physical sufficiency was evaluated via the survey which was composed of 11 items related to the daily activities (16, 17). The questions were aiming to highlight well-being and the loss of daily work, difficulty in working, pain, fatigue, and well-being in the morning after waking up, stiffness, anxiety, and depression. High scores presented functional limitations.

PITTSBURGH SLEEPING QUALITY SCALE

Buysse et al. developed the PSQS. The PSQS scale mainly evaluates the sleep quality, the amount of sleep, and sleep disturbances (18). The Turkish validity and reliability study of this study was conducted by Agargun et al. (19). The scale is composed of 19 questions and it is scored between 0 and 3. PSQS is composed of seven sub-dimensions such as subjective sleep quality, sleep latency, sleep duration, sleep adequacy, sleep disturbances, the use of sleeping pills, and days of dysfunction. High scores reflect the low sleep quality (18).

BIOCHEMICAL ANALYSIS

Venous blood samples of all individuals were collected into a dry tube after 10–12 hours of fasting and after 30 minutes of rest. All the blood samples were collected between 8 am and 9 am under the same conditions. Blood samples were centrifuged at 1000 g for 15 minutes right after they were taken. Serum samples were separated into different tubes and they were stored at –80 °C for the analyses. Complete blood count examined via flow cytometry technique (Mindray BC-6800 Auto Hematology Analyzer, Shenzhen, China); C-reactive protein (CRP), ALT and creatinine tests

were performed by spectrophotometric method (Abbot-Architect c8000, Japan); and erythrocyte sedimentation rate (ESR) was measured by Westergren method (Berkhum SDM-100, Turkey). Analyses were performed in the biochemistry laboratory of the Malatya State Hospital.

THIOL/DISULFIDE MEASUREMENT

Serum native thiol (NT), total thiol (TT) and disulfide levels (μmol/L) were measured by the method which was developed by Erel et al. (14) Disulfide/native thiol (DNT), disulfide/total thiol (DTT) and native thiol/total thiol (NTT) rates were calculated (%). In the presence of the sodium borohydride, disulfide bonds were reduced to functional thiol groups particularly. Then, the sodium borohydride was removed with the help of formaldehyde. Reduced and NT groups were measured after the 5,5′-dithiobis- (2-nitrobenzoic) acid (DTNB) reaction. (Disulfide amount was calculated by dividing the difference between TT and NT by two.

STATISTICAL ANALYSIS

The results were given as mean ± SD and median (range). SPSS program (version 18, IBM, Chicago, IL, USA) was used for the statistical analysis. The homogeneity of the distribution of the groups was evaluated by Kolmogorov Smirnov test. Student's t-test was used for the data with normal distribution, the non-homogenous data such as ESR, CRP and pain duration were analyzed with Mann Whitney-U test. Categorical data were evaluated by chi-square test. Pearson correlation test was used for correlation analysis. A p value of < 0.05 was considered significant.

RESULTS

FIQ scores, number of sensitive points, and duration of pain were higher in FMS patients when compared to the controls ($p < 0.001$). In Table 1, sociodemographic characteristics, working status, medications, and clinical findings are given.

NT ($p = 0.005$) and NTT ($p < 0.001$) values of FMS patients were higher when compared to healthy controls. Similarly, disulfide ($p < 0.001$), DNT ($p < 0.001$) and DTT ($p < 0.001$) values were also higher in FMS patients compared to the controls. CRP and ESR values of FMS patients were found similar to the control group values. Thiol, disulfide and other biochemical findings of FMS patients are

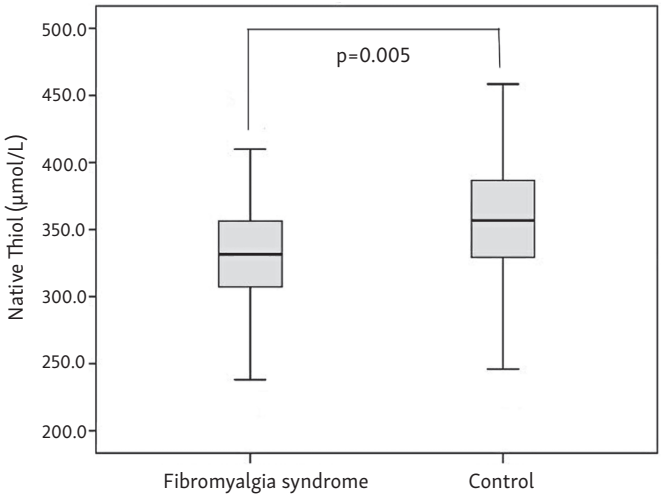

Fig. 1 Native thiol in Fibromyalgia syndrome.

Tab. 1 Demographic and clinic features of patients and control group.

	Fibromyalgia (n = 80) (mean ± SD)	Control (n = 64) (mean ± SD)	P value
Age (years)	41.4 ± 7.6	39.9 ± 10.9	0.341
BMI (kg/m^2)	26.7 ± 3.7	26.5 ± 5.6	0.811
Occupation (housewife/working) (n)	46/34	36/28	0.234
Pain duration (years) (median [range])	3.0 (0.5–20.0)	0.4 (0–9.0)	0.001
FIQ score	68.6 ± 11.1	36.2 ± 23.7	0.001
Number of *sensitive* points (n)	13.7 ± 2.8	1.0 ± 1.4	0.001
PSQS	7.5 ± 3.7	3.8 ± 3.2	0.001
SSRI (n)	33	0	0.001
MAOIs (n)	5	0	0.001
Pregabalin (n)	24	0	0.001
Gabapentin (n)	5	0	0.001
NSAIDs without other drugs (n)	13	0	0.001
NSAIDs with other drugs (n)	37	0	0.001
Opioids (n)	0	0	1.000
Cannabinoids (n)	0	0	1.000
Contraceptives (n)	0	0	1.000

Abbreviations: BMI – body mass index; FIQ – Fibromyalgia Impact Questionnaire; PSQS – Pittsburgh Sleeping Quality Scale; SSRI – selective serotonin reuptake inhibitor; MAOIs – monoamine oxidase inhibitors; NSAIDs – non-steroidal anti-inflammatory drugs.

Tab. 2 Results of thiol, disulfide and biochemical parameters in fibromyalgia and control groups.

	Fibromyalgia (n =8 0) (mean ± SD)	Control (n = 64) (mean ± SD)	P value
Native Thiol (µmol/L)	330.6 ± 46.1	356.8 ± 55.5	0.005
Total Thiol (µmol/L)	369.5 ± 49.0	381.3 ± 51.3	0.183
Native thiol/total thiol ×100	89.4 ± 3.2	93.3 ± 4.0	0.001
Disulfide (µmol/L)	19.4 ± 6.3	12.2 ± 6.3	0.001
Disulfide/native thiol ×100	5.9 ± 2.0	3.6 ± 2.5	0.001
Disulfide/total thiol ×100	5.2 ± 1.6	3.3 ± 2.0	0.001
BUN (mg/dl)	12.9 ± 1.2	13.3 ± 1.1	0.062
Creatinine (mg/dl)	0.7 ± 0.4	0.7 ± 0.1	0.454
AST (IU/l)	17.9 ± 6.4	19.5 ± 8.0	0.201
ALT (IU/l)	17.4 ± 10.5	19.4 ± 9.7	0.237
HB (g/dl)	12.9 ± 1.2	13.3 ± 1.1	0.062
CRP (mg/dl) (median [range])	0.3 (0–14.0)	0.3 (0–4.3)	0.480
ESR (mm/h)	15.1 ± 8.3	15.5 ± 9.3	0.817

Abbreviations: BUN – blood urea nitrogen; AST – aspartate aminotransferase; ALT – alanine aminotransferase; CRP – C-reactive protein; ESR – erythrocyte sedimentation rate.

given in Table 2. The NT levels are shown in Figure 1 and disulfide levels are shown in Figure 2.

There was a positive correlation between FIQ and BMI (r = 0.227, p = 0.006) and age (r = 0.240, p = 0.004). In our study, there was not any correlation between CRP, ESR and FIQ, number of sensitive points, and duration of pain, thiol, and disulfide levels. There was a negative correlation between FIQ scores and NTT levels. We found a positive relationship between FIQ scores and disulfide, DNT and DTT values. There was a negative correlation between the number of sensitive points and NT and NTT levels while a positive correlation between D, DNT, and DTT was found. There was a positive relationship between the pain duration and disulfide values. FIQ scores, number of sensitive points and pain duration and thiol and disulfide levels had positive correlations. Results are given in Table 3. Correlation between disulfide and FIQ score is shown in Figure 3. Additionally, there was a negative correlation between PSQS and NT (r = –0.211, p = 0.012), TT (r = –0.170, p = 0.043) and NTT (r = –0.190, p = 0.023). However, we found a positive correlation between PSQS scores and disulfide (r = 0.166, p = 0.048), DNT (r = 0.172, p = 0.040) and DTT (r = 0.193, p = 0.021).

DISCUSSION

The thiol levels of FMS patients were lower and the disulfide levels of patients were higher compared to control individuals. There was a significant relationship between thiol levels and FIQ scores, the number of sensitive points, and PSQS scores. FMS is commonly observed in women and it is characterized by a widespread pain. However, the etiology of FMS has not yet been clarified. FMS is associated with increased oxidative stress, widespread pain, fatigue and depression (20, 21). Chronic inflammation and

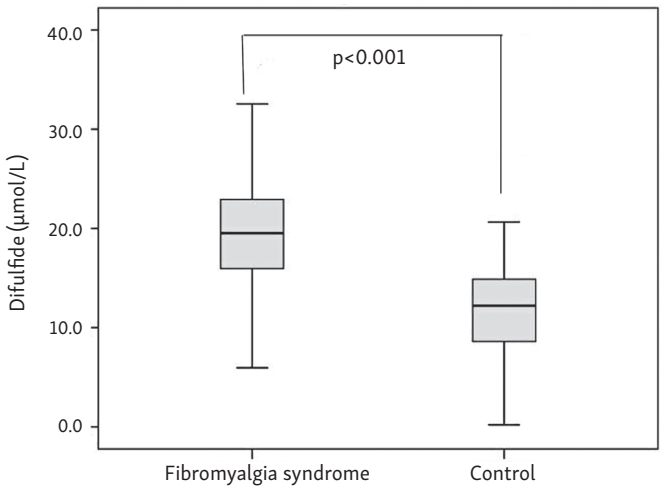

Fig. 2 Disulfide levels in Fibromyalgia syndrome.

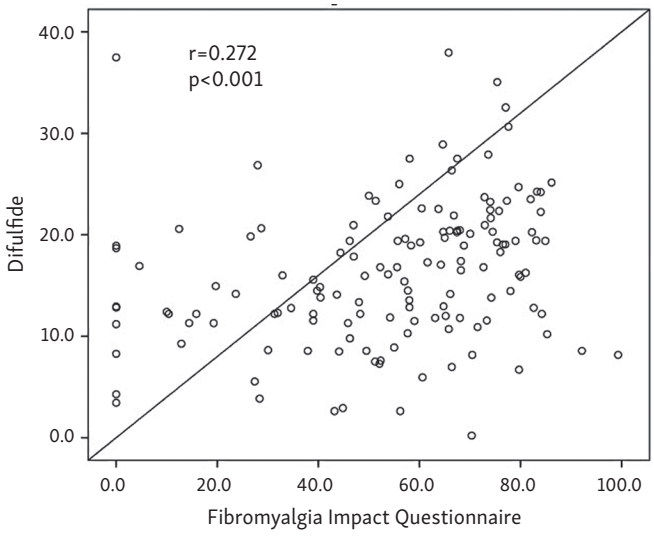

Fig. 3 Correlation between disulfide and FIQ score.

Tab. 3 Results of thiol, disulfide and other parameters for correlation analysis in fibromyalgia.

	FIQ score		Number of sensitive points		Pain duration	
	r value	p value	r value	p value	r value	p value
Native Thiol	-0.142	0.091	-0.267	0.001	-0.080	0.341
Total Thiol	-0.068	0.421	-0.133	0.113	-0.024	0.778
Native Thiol/Total Thiol	-0.240	0.004	-0.476	0.001	-0.164	0.051
Disulfide	0.272	0.001	0.492	0.001	0.204	0.015
Disulfide/Native Thiol	0.220	0.008	0.451	0.001	0.149	0.075
Disulfide/Total Thiol	0.240	0.004	0.475	0.001	0.164	0.050
Number of sensitive points	0.684	0.001			0.417	0.001
Pain Duration	0.396	0.001	0.417	0.001		

Abbreviations: FIQ, Fibromyalgia Impact Questionnaire.

oxidative stress can cause deterioration in the hypothalamic-pituitary-adrenal axis and thus FMS can occur (22). Oxidative stress can lead to mitochondrial damage and the deterioration of the energy balance and antioxidant defense system by affecting the protein kinases. Mitochondrial damage also takes place in FMS etiopathogenesis (23, 24). In the study of Neval et al., it was shown that total oxidant status and oxidative stress status were higher and total antioxidant status was lower in FMS patients when compared to the controls (25). The study by Fatima et al. showed that lipid peroxidation levels of FMS patients were higher and levels of antioxidant defense system enzymes such as glutathione peroxidase (GPx) and glutathione reductase in FMS patients were lower than the controls (21). However, there are studies stating that oxidant and antioxidant capacity of FMS patients were similar with the control group. Akbas et al. showed that GPx enzyme levels were similar in both FMS patients and healthy individuals (26, 27). Similarly, Toker et al. indicated that the ischemia-modified albumin levels were also similar in FMS patients and controls (26). Bozkurt et al. found that the oxidant status and oxidative stress index values of FMS patients were higher than controls but total antioxidant status and paraoxonase-1 levels were similar in patients and controls (28). Regarding these results, there are contradictory findings in the literature.

Glutathione is a tripeptide containing thiol and it protects the organism from the oxidative stress by activity of the enzyme GPx (29). In many studies, instead of studying the direct thiol group, glutathione and GPx levels were studied. Many drugs have a positive or negative effect on thiol levels (30). Our patients used selective serotonin reuptake inhibitors (SSRIs), monoamine oxidase inhibitors (MAOIs), non-steroidal anti-inflammatory drugs (NSAIDs), pregabalin and gabapentin. SSRIs are found to increase GPx, glutathione and thiol levels in the brain tissue while they cause a severe decrease in GPx, glutathione and thiol levels in the liver tissue (31). It has been reported that pregabalin, gabapentin, and NSAIDs decrease GPx levels (30–33). The low level of GPx and glutathione indirectly indicates the low thiol levels. In this study, low thiol levels in FMS patients may be due to the use of these drugs.

It was shown by Sarifakioglu et al. that there was a strong relationship between the oxidative stress parameters and FIQ, Beck depression inventory and visual analog scale scores (34). In our study, there was a strong positive relationship between thiol levels of FMS patients and their FIQ scores, number of sensitive points and the PSQS. On the other hand, we found a negative correlation between disulfide levels and FIQ scores, sensitive points, and the PSQS. Thiols have roles in the maintenance of the oxidative balance and they are molecules that contain sulfhydryl groups (10). Thiols create disulfide bonds in the presence of oxygen via oxidation (12). Thiols are mainly present in albumin and other protein derives such as cysteine, methionine, and reduced glutathione (35). Thiols have important roles in the clearance of hypochlorous acid from the body (36). It shows that oxidative stress increases due to the low thiol levels and high disulfide levels. The plasma thiol measurement was previously performed by using old manual methods (37). However, Erel et al. have recently found a cheap, easy, reliable, and fully automated method and the thiol/disulfide balance can be measured by using this technique (14). Using this method revealed that the balance of thiol/disulfide was deteriorated in favor of the disulfide in diseases such as Familial Mediterranean fever, cardiac disease and diabetes mellitus which are characterized with an enhanced oxidative stress (13, 38, 39). In our study, we showed that FMS patients have lower thiol levels and higher disulfide levels compared to controls. In FMS patients, there was a strong relationship between the number of sensitive points and the thiol/disulfide levels. Furthermore, the sleeping status and the thiol levels of the patients had a relationship. Our findings lead us to think that thiol/disulfide balance is deteriorated in FMS and oxidative stress has a role in the etiology of this disease.

In our study, CRP levels of our patients were not high and there was no correlation between the CRP levels and thiol levels of patients. CRP is a good indicator of inflammation. However, fibromyalgia is not an inflammation-related disease and CRP increase is not expected in the course (3). Xiao et al. showed that high sensitive (hs)-CRP levels were higher in FMS patients when compared to controls (40). However, patient and control groups were not matched regarding BMI-matched; FMS patients and controls had prominent weight difference. The group found that hs-CRP increased even though the

inflammation status was low. Rus et al. showed that both normal and the over-weighted FMS patients had higher CRP levels compared to the controls. However, a relationship was present between CRP levels and disease activity of the over-weighted FMS patients (41). Rus et al. had a smaller sample size and it is possible that the results might be affected due to the sample size. Xiao et al. and Rus et al. reported high CRP levels in obese FMS patients. It is well known that obesity causes inflammation. Therefore, studies of Xiao et al. and Rus et al. may found high CRP levels in FMS patients due to the obesity status of individuals rather than the disease. CRP is mostly secreted from the liver and CRP release is mainly induced by interleukin-6 (IL)-6. If the IL-6 release is low or if there is a lack of response against IL-6, CRP levels may not increase (42). It is known that IL-6 levels are not increased in FMS and both patients and the controls have similar levels of IL-6 cytokine (43, 44). In our study, we found similar levels of CRP in both the patient group and the control group most probably due to the lack of increase in IL-6 levels. Furthermore, increased cytokine level increases the oxidative stress but cytokine release is not required for the formation of the oxidative stress (45). This can be the reason why we could not reveal any relationship between CRP levels and thiol groups.

As a result, this study concluded that thiol levels were lower and disulfide levels were higher in FMS patients when compared to the controls. The change in the thiol/disulfide balance in favor of disulfide amounts reflects the oxidative stress. Increased oxidative stress can have a role in the deterioration of the thiol balance in FMS patients. It is possible to examine whether or not drugs with thiol groups have positive effects on FMS patients.

REFERENCES

1. Bennett RM, Jones J, Turk DC, Russell IJ, Matallana L. An internet survey of 2,596 people with fibromyalgia. BMC Musculoskelet Disord 2007; 8: 27.
2. Couto CI, Natour J, Carvalho AB. Fibromyalgia: its prevalence and impact on the quality of life on a hemodialyzed population. Hemodial Int 2008; 12: 66–72.
3. Arnold LM, Clauw DJ, McCarberg BH. FibroCollaborative. Improving the recognition and diagnosis of fibromyalgia. Mayo Clin Proc 2011; 86: 457–64.
4. Cohen H, Neumann L, Glazer Y, Ebstein RP, Buskila D. The relationship between a common catechol-O-methyltransferase (COMT) polymorphism val (158) met and fibromyalgia. Clin Exp Rheumatol 2009; 27: 51–6.
5. Wallace DJ, Linker-Israeli M, Hallegua D, Silverman S, Silver D, Weisman MH. Cytokines play an aetiopathogenetic role in fibromyalgia: a hypothesis and pilot study. Rheumatology (Oxford) 2001; 40: 743–9.
6. Kato K, Sullivan PF, Evengard B, Pedersen NL. Importance of genetic influences on chronic widespread pain. Arthritis Rheum 2006; 54: 1682–6.
7. Ozgocmen S, Ozyurt H, Sogut S, Akyol O. Current concepts in the pathophysiology of fibromyalgia: the potential role of oxidative stress and nitric oxide. Rheumatol Int 2006; 26: 585–97.
8. Altindag O, Celik H. Total antioxidant capacity and the severity of the pain in patients with fibromyalgia. Redox Rep 2006; 11: 131–5.
9. Cordero MD, de Miguel M, Carmona-Lopez I, Bonal P, Campa F, Moreno-Fernandez AM. Oxidative stress and mitochondrial dysfunction in fibromyalgia. Neuro Endocrinol Lett 2010; 31: 169–73.
10. Altiparmak IH, Erkus ME, Sezen H, et al. Evaluation of thiol levels, thiol/disulfide homeostasis and their relation with inflammation in cardiac syndrome X. Coron Artery Dis 2016; 27: 295–301.
11. Jovanovic VB, Pavicevic ID, Takic MM, Penezic-Romanjuk AZ, Acimovic JM, Mandic LM. The influence of fatty acids on determination of human serum albumin thiol group. Anal Biochem 2014; 448: 50–7.
12. Yuksel M, Ates I, Kaplan M, et al. The dynamic thiol/disulphide homeostasis in inflammatory bowel disease and its relation with disease activity and pathogenesis. Int J Colorectal Dis 2016; 31: 1229–31.
13. Kundi H, Ates I, Kiziltunc E, et al. A novel oxidative stress marker in acute myocardial infarction; thiol/disulphide homeostasis. Am J Emerg Med 2015; 33: 1567–71.
14. Erel O, Neselioglu S. A novel and automated assay for thiol/disulphide homeostasis. Clin Biochem 2014; 47: 326–32.
15. Wolfe F, Clauw DJ, Fitzcharles MA, et al. The American College of Rheumatology preliminary diagnostic criteria for fibromyalgia and measurement of symptom severity. Arthritis Care Res (Hoboken) 2010; 62: 600–10.
16. Burckhardt CS, Clark SR, Bennett RM. The fibromyalgia impact questionnaire: development and validation. J Rheumatol 1991; 18: 728–33.
17. Sarmer S, Ergin S, Yavuzer G. The validity and reliability of the Turkish version of the Fibromyalgia Impact Questionnaire. Rheumatol Int 2000; 20: 9–12.
18. Buysse DJ, Reynolds CF 3rd, Monk TH, Berman SR, Kupfer DJ. The Pittsburgh Sleep Quality Index: a new instrument for psychiatric practice and research. Psychiatry Res 1989; 28: 193–213.
19. Ağargün MY, Kara H, Anlar Ö. Pittsburgh Uyku Kalitesi İndeksi›nin geçerliği ve güvenirliği. Turk Psikiyatr Derg 1996; 7: 107–15.
20. Peres Klein C, Rodrigues Cintra M, Binda N, et al. Coadministration of Resveratrol and Rice Oil Mitigates Nociception and Oxidative State in a Mouse Fibromyalgia-Like Model. Pain Res Treat 2016; 2016: 3191638.
21. Fatima G, Das SK, Mahdi AA. Some oxidative and antioxidative parameters and their relationship with clinical symptoms in women with fibromyalgia syndrome. Int J Rheum 2017; 20: 39–45.
22. Romano GF, Tomassi S, Russell A, Mondelli V, Pariante CM. Fibromyalgia and chronic fatigue: the underlying biology and related theoretical issues. Adv Psychosom Med 2015; 34: 61–77.
23. Alcocer-Gomez E, Garrido-Maraver J, Bullon P, et al. Metformin and caloric restriction induce an AMPK-dependent restoration of mitochondrial dysfunction in fibroblasts from Fibromyalgia patients. Biochim Biophys Acta 2015; 1852: 1257–67.
24. Sanchez-Dominguez B, Bullon P, Roman-Malo L, et al. Oxidative stress, mitochondrial dysfunction and, inflammation common events in skin of patients with Fibromyalgia. Mitochondrion 2015; 21: 69–75.
25. Neyal M, Yimenicioglu F, Aydeniz A, et al. Plasma nitrite levels, total antioxidant status, total oxidant status, and oxidative stress index in patients with tension-type headache and fibromyalgia. Clin Neurol Neurosurg 2013; 115: 736–40.
26. Toker A, Kucuksen S, Kucuk A, Cicekler H. Serum ischemia-modified albumin and malondialdehyde levels and superoxide dismutase activity in patients with fibromyalgia. Clin Lab 2014; 60: 1609–15.
27. Akbas A, Inanir A, Benli I, Onder Y, Aydogan L.Evaluation of some antioxidant enzyme activities (SOD and GPX) and their polymorphisms (MnSOD2 Ala9Val, GPX1 Pro198Leu) in fibromyalgia. Eur Rev Med Pharmacol Sci 2014; 18: 1199–203.
28. Bozkurt M, Caglayan M, Oktayoglu P, et al. Serum prolidase enzyme activity and oxidative status in patients with fibromyalgia. Redox Rep 2014; 19: 148–53.
29. Dickinson DA, Forman HJ. Cellular glutathione and thiols metabolism. Biochem Pharmacol 2002; 64: 1019–26.
30. Wolf WA, Kuhn DM. Role of essential sulfhydryl groups in drug interactions at the neuronal 5-HT transporter. Differences between amphetamines and 5-HT uptake inhibitors. J Biol Chem 1992; 267: 20820–5.
31. Abdel Salam OM, Mohammed NA, Sleem AA, Farrag AR. The effect of antidepressant drugs on thioacetamide-induced oxidative stress. Eur Rev Med Pharmacol Sci 2013; 17: 735–44.
32. Erdemir F, Atilgan D, Firat F, Markoc F, Parlaktas BS, Sogut E. The effect of sertraline, paroxetine, fluoxetine and escitalopram on testicular tissue and oxidative stress parameters in rats. Int Braz J Urol 2014; 40: 100–8.
33. Abdel-Salam OM, Khadrawy YA, Mohammed NA, Youness ER. The effect of gabapentin on oxidative stress in a model of toxic demyelination in rat brain. J Basic Clin Physiol Pharmacol 2012; 23: 61–8.
34. Sarıfakıoğlu B, Güzelant AY, Güzel EC, Güzel S, Kızıler AR. Effects of 12-week combined exercise therapy on oxidative stress in female fibromyalgia patients. Rheumatol Int 2014; 34: 1361–7.
35. Turell L, Radi R, Alvarez B. The thiol pool in human plasma: the central contribution of albumin to redox processes. Free Radic Biol Med 2013; 65: 244–53.
36. Storkey C, Davies MJ, Pattison DI. Reevaluation of the rate constants for the reaction of hypochlorous acid (HOCl) with cysteine, methi-

onine, and peptide derivatives using a new competition kinetic approach. Free Radic Biol Med 2014; 73: 60–6.
37. Ellman GL, Lysko H. Disulfide and sulfhydryl compounds in TCA extracts of human blood and plasma. J Lab Clin Med 1967; 70: 518–27.
38. Ates I, Kaplan M, Yuksel M, et al. Determination of thiol/disulphide homeostasis in type 1 diabetes mellitus and the factors associated with thiol oxidation. Endocrine 2016; 51: 47–51.
39. Yucel A, Sanhal CY, Daglar K, Kara O, Uygur D, Erel O. Thiol/disulphide homeostasis in pregnant women with Familial Mediterranean fever. Redox Rep 2016; 21: 287–91.
40. Xiao Y, Haynes WL, Michalek JE, Russell IJ. Elevated serum high-sensitivity C-reactive protein levels in fibromyalgia syndrome patients correlate with body mass index, interleukin-6, interleukin-8, erythrocyte sedimentation rate. Rheumatol Int 2013; 33: 1259–64.
41. Rus A, Molina F, Gasso M, Camacho MV, Peinado MA, Moral ML. Nitric Oxide, Inflammation, Lipid Profile, and Cortisol in Normal- and Overweight Women With Fibromyalgia. Biol Res Nurs 2016; 18: 138–46.
42. Puel A, Picard C, Lorrot M, et al. Recurrent staphylococcal cellulitis and subcutaneous abscesses in a child with autoantibodies against IL-6. J Immunol 2008; 180: 647–54.
43. Fatima G, Mahdi AA, Das SK, et al. Lack of Circadian Pattern of Serum TNF-α and IL-6 in Patients with Fibromyalgia Syndrome. Indian J Clin Biochem 2012; 27: 340–3.
44. Ghizal F, Das SK, Verma N, Mahdi AA. Evaluating relationship in cytokines level, Fibromyalgia Impact Questionnaire and Body Mass Index in women with Fibromyalgia syndrome. J Back Musculoskelet Rehabil 2016; 29: 145–9.
45. Gebicki JM. Oxidative stress, free radicals and protein peroxides. Arch Biochem Biophys 2016; 29: 145–9.

Nightstick Fractures, Outcomes of Operative and Non-Operative Treatment

Mohammed Ali*, D. I. Clark, Amole Tambe

ABSTRACT

Introduction: A nightstick fracture is an isolated fracture of the ulnar shaft. Although operative and non-operative treatments have been commonly decided by the degree of displacement of the fracture, still there is a controversy specially in those moderately displaced. Herein we report our experience with nightstick fractures.

Objective: To evaluate operative and non-operative treatment of nightstick fracture.

Materials and methods: We retrospectively reviewed the clinical notes, physiotherapy letters and radiographs of 52 patients with isolated ulnar shaft fractures. Outcome Measurements included radiographic healing, post-operative range of motion and complications.

Results: The study included 13 females and 39 males, with a mean age of 26 years [range, 18–93 years]. The mean Follow-up period was 32 months ranged from 12 to 54 months. Ten patients were treated non-operatively; forty-two patients had open reduction and internal fixation including six open fractures. The average wait for surgery was 2.5 days. Mobilisation was commenced immediately after the surgeries non-load bearing. 40 patients had no complications post-operatively with good outcome and average of four visits follow-up. In the non-operative group, five out ten failed and had a mean follow-up of nine visits.

Conclusion: Satisfactory outcome is to be expected with open reduction and internal fixation. Fractures with less than 50% displacement should be treated on individual bases, considering; age, pre-morbid functional status, co-morbidities, compliance and associated injuries.

KEYWORDS

nightstick fracture; ulnar shaft fracture; non-operative management; non-union

AUTHOR AFFILIATIONS

Royal Derby Hospital, Derby, United Kingdom

* Corresponding author: Trauma and Orthopaedics Department, South Tyneside District Hospital, Harton Ln, South Shields NE34 0PL, United Kingdom; e-mail: mohammedkhider84@hotmail.com

Received: 14 January 2018
Accepted: 8 November 2018
Published online: 1 April 2019

Acta Medica (Hradec Králové) 2019; 62(1): 19–23
https://doi.org/10.14712/18059694.2019.41

INTRODUCTION

A nightstick fracture is an isolated fracture of the ulnar shaft (IUSF) associated with a direct blow usually as a result of the forearm being held in protection across the face (1). It can also occur with excessive supination or pronation. In these fractures, the integrity of the periosteum and the interosseous membrane determines the stability of the fracture and this is normally indicated by the initial displacement. Although typically closed fractures, they have a higher rate of delayed union or non-union. The aim of management is to prevent the complications of malunion and non-union and restore the best possible function of the limb. Majority of nightstick fractures used to be treated non-operatively (1) and numerous methods of immobilisation have been adopted by surgeons. However, the treatment of isolated ulnar fractures remains controversial, with different authors advocating both surgical and non- surgical management. Herein we report our experience with nightstick fractures.

METHODS

Retrospectively, we reviewed 96 consecutive patients with ulnar shaft fractures admitted to our hospital from September 2010 to December 2015. The study comprised review of patients' clinical notes and radiographs. Ulnar shaft fractures with ipsilateral radial, humeral, or wrist fractures were excluded. Add to that, Monteggia fractures were excluded, as were fractures of the olecranon or coronoid or styloid processes. These fractures resulted from assaults with a stick like weapon, road accidents or falls. 52 patients met the inclusion criteria. The method of treatment was decided by the treating surgeon. Part of these fractures was treated with open reduction and internal fixation using plates and the other part were treated closed with an above elbow arm cast.

We also reviewed the site of these fractures (proximal, middle, or distal shaft) and the degree of displacement.

Surgeries were performed either under general anaesthesia with local anaesthetic infiltration or regional block. Patients were placed in a supine position with the arm placed on an upholstered arm-board. Pneumatic tourniquet was used in all cases. An ulnar approach to the ulnar shaft was performed in all operative cases.

For antimicrobial prophylaxis, Cefuroxime was used intravenously, with 1.5 g injected intra-operatively and 0.75 g injected after 8 and 16 hours. The operated arm of all patients had a wool and crepe dressing and put in a broad arm sling post-operatively.

Patients started gentle wrist and shoulder movement non-load bearing immediately after surgery. Patients then seen after two weeks in outpatient clinics, where they had a wound check and started gentle elbow exercise including active pronation/ supination movement. All patients had post-operative physiotherapy referral initiated at two weeks as per our hospital protocol. Reduction and fixation were checked with plane radiographs at two weeks, six and 12 weeks post-operatively. Based on the progress with the physiotherapy and the bony union on the radiographs they either discharged with an open appointment or given further follow-up appointment.

In the non-operative group; immobilisation was obtained through an above elbow back-slab in a mid-prone position with the elbow in 90 degrees flexion and the wrist in a neutral position. After one week, patients had a repeat radiograph to check the position of the fracture. The back-slab was then either completed or converted to a full cast at one week if the fracture position still acceptable. Patients had x-rays at two and four weeks in view of late slipping. Patients also had x-rays at 8 weeks and when there was good evidence of healing, cast was removed they were referred to physiotherapy. At 12 weeks, they will be reviewed again with plain radiographs to assess the healing of the fracture specially if patients are symptomatic.

Upon review, fracture union was considered when there is a bridging callus with no tenderness or movement at the fracture site. Non-union was declared when there was evidence of hypertrophic callus without bridging and persistent pain at the fracture site.

RESULTS

52 cases were found to be isolated ulnar shaft fractures. This included 13 females and 39 males, with a mean age of 26 years [range, 18–93 years]. The mean Follow-up period was 32 months ranged from 12 months to 54 months. One patient had proximal third shaft fracture, 12 patients had distal shaft fractures and 39 patients demonstrated mid shaft fractures. 16 fractures were comminuted, 22 oblique displaced fractures, 13 transverse displaced fractures, one un-displaced transverse fracture. 6 patients had Open fractures.

THE OPERATIVE GROUP

42 patients had open reduction and internal fixation using plate and screw fixation, this group included six open fractures. 38 fractures were fixed using a dynamic compression plate (DCP) and four with a limited contact dynamic compression plate (LC-DCP) (Figure 1). The mean waiting time for surgery was 2.5 days, ranging from 1 to 7 days.

None developed wound infection or wound breakdown post-operatively. There were no recorded instances of nerve damage.

Adequate union was achieved in 40 (95%) cases. Two patients (5%) after DCP fixation, developed non-union during the follow-up (20 and 24 weeks) period and required a revision surgery (Figure 2). Fixation in both cases was done after anatomical reduction. Both patients had uneventful early post-operative course however one patient was reported to be a smoker and the other patient we could not find any mechanical or biological reason for the non-union.

In the 42 surgical cases; Anatomical reduction from time of surgery was maintained in all patients during follow-up. All patients were reported to have full supination, pronation and mean flexion arc of 10 to 130 degrees (+/– 10) at 12 Week. Good callus formation was noted in 40 patients at 12 weeks. No reported cases of mal-union or

Fig. 1 x-rays show anatomical reduction of the fracture and fixation using plate and screws.

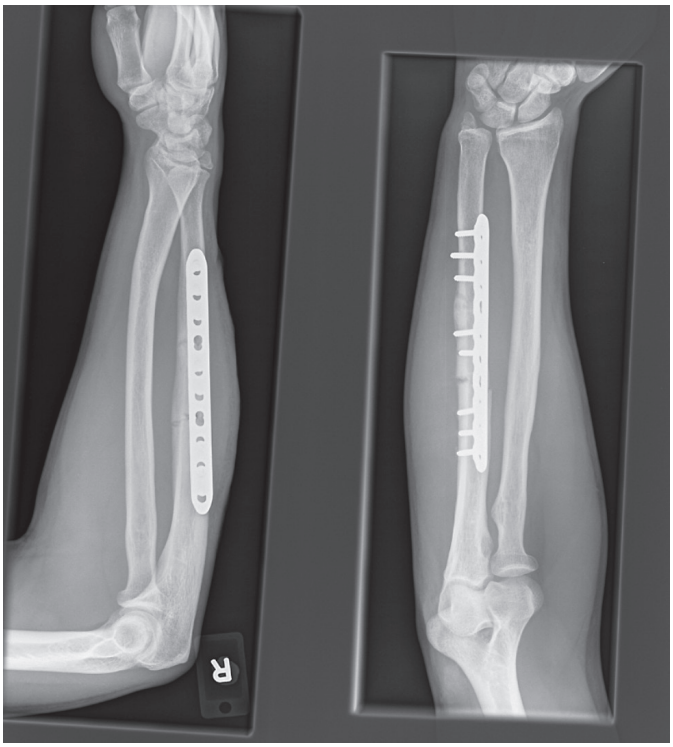

Fig. 2 X-rays show revision of a non-united fracture.

metal work failure. Only one patient was reported to develop metal work irritation from a DCP plate and required a metal work removal after 6 months. The average number of hospital visits was 4 (ranged from 4 to 6 visits).

THE NON-OPERATIVE GROUP

Ten patients were treated non-operatively (Table 1). Five patients were declared to fail non-operative treatment. One patient developed a mal-union however; he was happy with the function and did not want to go down the surgical route. At two weeks, four patients had further displacement beyond the acceptable limits. Three of them had a surgical fixation after two weeks and one patient was deemed not to be fit for surgery and went into non-union. The average number of hospital visits was 9 (ranged from 7 to 10 visits).

The other five patients had above elbow plaster cast in a mid-prone position. Cast was reduced to below elbow at 4 weeks and removed at eight weeks. Patients were then referred to physiotherapy. At 12 weeks, they were reviewed again with plain radiographs and fractures deemed to be

Tab. 1 Patients who received non-operative treatment.

Age/sex	ASA	PMH	Smoking	Fracture	Treatment	Complications
73/M	4	IHD, OP	No	Mid-shaft disp-oblique	Above elbow casting	Non-union
49/M	1	None	No	Mid-shaft comminuted	Above elbow casting	None
89/M	4	OP, IHD, CKD	No	Mid-shaft comminuted	Above elbow casting	None
35/F	1	None	No	Distal third disp-oblique	Above elbow casting	None
21/M	1	None	Yes	Distal third disp-oblique	Above elbow casting / ORIF	Further displacement beyond acceptable limit
73/M	2	PVD, OP	No	Mid-shaft disp-trans	Above elbow casting	None
59/F	3	CKD, OP	No	Mid-shaft disp-trans	Above elbow casting	None
51/F	1	None	No	Distal third disp-trans	Above elbow casting / ORIF	Further displacement beyond acceptable limit
32/M	1	None	No	Mid-shaft disp-trans	MUA / Above elbow casting	Mal-union
18/M	1	None	No	Mid-shaft undisp-trans	Above elbow casting / ORIF	Further displacement beyond acceptable limit

united based on radiographs and clinical examination. Patients were reported to have (–5 degrees) from full supination and pronation and mean flexion arc of 10 to 120 degrees (+/– 10). At 12 weeks, all were discharged to the care of the physiotherapy and left with an open appointment should they have any problems in the future.

DISCUSSION

Non-operative treatment has been embraced by many authors and traditionally, benign neglect or non-operative management was reported to give satisfactory results with a prompt return to function and good healing rates. Traditionally, non-operative treatment was mainly recommended for non-displaced fractures or fractures with less than 50% displacement (2–4). The 1984 paper by Dymond et al. (5) which was authored based on a cadaveric study, concluded that more than 50% displacement involves considerable disruption of the periosteum and of the interosseous membrane. These displaced fractures were deemed to be unstable and necessitate above-elbow immobilisation for stability. In a minimally displaced ulnar shaft fracture, these structures, together with the intact radius, provide a strong stabilizing effect, which may explain why some authors (6, 7) were able to achieve satisfactory outcomes by treating low-energy ulnar fractures with minimum immobilization (8, 9). Furthermore, two studies have concluded that minimally displaced IUSFs in the middle and distal third of the ulna are stable and can be mobilised at earlier stages (10, 11). On the other hand, some authors suggested that proximal IUSF are best treated by ORIF, believing that the soft-tissue forces tend to destabilize fractures in this region. Also, it is possible that some of these are occult Monteggia fractures that have spontaneously reduced (9, 10). Hopper and Sarmiento although they advised non-operative treatment for diaphysial fractures in the distal two thirds, they excluded those in which the bone ends are displaced by 5 mm or more and advised to be treated with open reduction and internal fixation, particularly if the mechanism of injury was high energy (2, 11). Riska and Nottage, shared the same views however, they excluded patients with head injury, spinal cord injury, or poly-trauma patient in whom internal fixation of distal two-thirds ulnar fractures may facilitate acute care or rehabilitation (12, 13). Szabo et al. (14) retrospectively reviewed the treatment and outcome of 46 isolated fractures of the ulnar shaft. 18 fractures had internal fixation and 28 were treated closed. One open fracture became infected following fixation and failed to unite. Seven failed the non-operative treatment and ended up with non-union. They suggested prognostic factors for non-union in non-operatively treated fractures which inclde; proximal third fractures and those with displacement 5 mm or more.

Immobilisation positions have been discussed as having a great role in maintaining fracture reduction and the eventual acceptable alignment of the healed fracture. Traditionally, recommendations for immobilizing the forearm in neutral, supination, or pronation positions have been based on theory, anecdotal experience, and tradition (15–18). A few clinical studies have shown success with the forearm immobilized in either pronation or supination (16, 18). Altner et al. (19) in their series, they immobilised patients in a mid-prone position and reported good results. Add to that Boyer et al. (20) evaluated the effect of forearm position on the healing outcomes following non-surgical treatment using above elbow cast. They concluded that residual fracture angulation at the time of union was not significantly affected by forearm position.

A review by Mackay (21) et al. in 2000, included 33 series involving 1876 patients. The outcomes of the non-surgical treatment of minimally displaced ulnar fractures with a stable configuration were consistently satisfactory. Below elbow plaster cast, functional brace and early mobilisation all achieved similar results. Above elbow cast was deemed to be unnecessarily restrictive. Mackay also concluded that open reduction and internal fixation is better used in widely displaced or unstable fractures to preserve the forearm rotation.

Moed et al. (22) Reported the outcomes of immediate internal plate fixation of an open diaphyseal fracture of the forearm in fifty patients. Although they had two cases of deep infection and non-union in six, the functional results were excellent or good in 85 per cent of the series. They related these results to the severity of the initial soft-tissue injury and the surgical technique and recommended autogenous cancellous bone-grafting in comminuted fractures. On the other hand, Wright et al. (23) studied 198 forearm fractures to determine the union rate where acute bone grafting was recommended but not performed. The overall union rate in comminuted, non-grafted forearm fractures (open and closed) was 98%. Another study by Wei et al. (24) concluded that acute bone grafting of diaphyseal forearm fractures did not affect the union rate or the time to union.

Recently, Cai and his fellow researchers (1) reviewed all published randomised controlled trials and observational studies that have assessed the outcome of these fractures following above- or below-elbow immobilisation, bracing and early mobilisation. They included 27 studies comprising 1629 fractures. They found that early mobilisation produced the shortest radiological union time and the lowest mean rate of non-union. They advised early mobilisation, with a removable forearm support for the treatment of nondisplaced or partially displaced nightstick fractures.

Coulibaly et al. in 2015 conducted a retrospective case-control analysis on patients diagnosed with IUSF to compare surgical and nonsurgical outcomes (25). They measured complications and functional ability. They found that nonsurgical treatment of IUSF is prone to complications and is associated with mal-union and non-union while Surgical treatment with rigid plate fixation and early range of motion resulted in a shorter period of cast immobilization and an earlier return to weight bearing, and led to reduced patient morbidity.

In our study, although the numbers are not comparable, complication rates in the non-operatively treated group were significantly higher than those reported in the operated group. In our study five fractures, Failed the non-operative treatment. Another notable correlate in

our series was location in the middle third of the shaft, an experience not shared in previous papers. Also, patients who developed these complications either were very young and might not be very compliant or elderly with multiple co-morbidities and this was also noted by Coulibaly.

The limitations of our study include its retrospective nature, the small number of patients and the relatively short duration of follow-up. There are other elements that we did not measure and that could have contributed to our conclusion.

CONCLUSION

Based on our study and the published literature we believe that IUSFs with more than 5 mm displacement should be treated operatively. Satisfactory outcome is to be expected with open reduction and internal fixation with rigid plate as it allows early mobilisation and enables earlier return to function with very low risk of wound problems. Although our study did not reveal good results with non-operative treatment, we believe those with less than 5 mm displacement should be treated on individual bases, considering; age, pre-morbid functional status, co-morbidities, compliance and associated injuries.

REFERENCES

1. Cai XZ, Yan SG, Giddins G. A systematic review of the non-operative treatment of nightstick fractures of the ulna. Bone Joint J 2013 Jul; 95-B(7): 952–9.
2. Hooper G. Isolated fractures of the shaft of the ulna. Injury 1974; 6(2): 180–4.
3. Du Toit FP, Grabe RP. Isolated fractures of the shaft of the ulna. S Afr Med I 1979; 56(1): 21–5.
4. Corea JR, Brakenbury PH, Blakemore ME. The treatment of isolated fractures of the ulnar shaft in adults. Injury 1981; 12(5): 365–70.
5. Dymond IW. The treatment of isolated fractures of the distal ulna. J Bone Joint Surg (Br) 1984; 66(3): 408–10.
6. Pollock FH, Pankovich AM, Prieto JJ, Lorenz M. The isolated fracture of the ulnar shaft. Treatment without immobilization. J Bone Joint Surg Am 1983; 65(3): 339–42.
7. Sarmiento A. Isolated ulnar shaft fractures treated with functional braces. J Orthop Trauma 1998; 12(6): 420–3.
8. Ekelund AL, Nilsson OS. Early mobilization of isolated ulnar shaft fractures. Acta Orthop Scand 1989; 60(3): 261–2.
9. de Jong T, de Jong PC. Ulnar shaft fracture needs no treatment. A pilot study of 10 cases. Acta Orthop Scand 1989; 60(3): 263–4.
10. Zych GA, Latta LL, Zagorski JB. Treatment of isolated ulnar shaft fractures with prefabricated functional fracture braces. Clin Orthop 1987; (219): 194–200.
11. Sarmiento A. Treatment of ulnar fractures by functional bracing. J Bone Joint Surg Am 1976; 58(8): 1104–7.
12. Nottage WM. A review of long bone fractures in patients with spinal cord injuries. Clin Orthop 1981; (155): 65–70.
13. Riska EB, von Bonsdorff H, Hakkinen S, Jaroma H, Kiviluoto O, Paavilainen T. Primary operative fixation of long bone fractures in patients with multiple injuries. J Trauma 1977; 17(2): 111–21.
14. Szabo RM, Skinner M. Isolated ulnar shaft fractures. Retrospective study of 46 cases. Acta Orthop Scand 1990 Aug; 61(4): 350–2.
15. Davis DR, Green DP. Forearm fractures in children. Clin Orthop 1976; 120: 172–84.
16. Evans EM. Rotational deformity in the treatment of fractures of both bones of the forearm. J Bone Joint Surg 1945; 27: 373–9.
17. Gibbons CLMH, Woods DA, Pailthorpe C, et al. The management of isolated distal radius fractures in children. J Pediatr Orthop 1994; 14: 207–10.
18. Gupta RP, Danielsson LG. Dorsally angulated solitary metaphyseal greenstick fractures in the distal radius: Results after immobilization in pronated, neutral, and supinated position. J Pediatr Orthop 1990; 10: 90–2
19. Altner, PC, Ted Hartman, J. Isolated Fractures of the Ulnar Shaft in the Adult. Surg Clin North Am 1972; 52(1): 155–70.
20. Boyer BA, Overton B, Schrader W, Riley P, Fleissner P. Position of Immobilization for Pediatric Forearm Fractures. J Pediatr Orthop 2002; 22(2): 185–7.
21. Mackay D, Wood L, Rangan A. The treatment of isolated ulnar fractures in adults: a systematic review. Injury 2000; 31(8): 565–70.
22. Moed BR, Kellam JF, Foster RJ, Tile M, Hansen ST Jr. Immediate internal fixation of open fractures of the diaphysis of the forearm. J Bone Joint Surg Am 1986 Sep; 68(7): 1008–17.
23. Wright RR, Schmeling GI, Schwab JP. The necessity of acute bone grafting in diaphyseal forearm fractures: a retrospective review. J Orthop Trauma 1997 May; 11(4): 288–94.
24. Wei SY, Born CT, Abene A, Ong A, Hayda R, DeLong WG Jr. Diaphyseal forearm fractures treated with and without bone graft. J Trauma 1999; 6: 1045–8
25. Coulibaly MO, Jones CB, Sietsema DL, Schildhauer TA. Results of 70 consecutive ulnar nightstick fractures. Injury 2015 Jul; 46(7): 1359–66.

Thoracic Radiography Characteristics of Drug Sensitive Tuberculosis and Multi Drug Resistant Tuberculosis: a Study of Indonesian National Tuberculosis Prevalence Survey

Rosalia Sri Sulistijawati[1], Aziza Ghanie Icksan[2], Dina Bisara Lolong[3], Fariz Nurwidya[4,*]

ABSTRACT

Background: Tuberculosis (TB) remains a burden globally, including Indonesia. The primary objective of this study is to reveal the chest radiography characteristic of drug-sensitive TB (DS-TB) and multi-drug resistant TB (MDR-TB) in the Indonesian national tuberculosis prevalence survey 2013–2014. The secondary objective is to explore the correlation and incidence rate of chest radiography lesion of DS-TB and MDR-TB cases.

Methods: This is a cross-sectional retrospective analytical studies with national and regional coverage. Samples were selected by stratified multi-stage clustering sampling technique in a population aged ≥15 years old. The diagnosis of TB was based on culture and GeneXpert tests.

Results: There were 147 DS-TB and 11 MDR-TB patients that were analyzed in this study. The nodule is the only type of lesions that distinguish MDR-TB and DS-TB. In multivariate analysis of DS-TB, there were 3 significant chest radiography lesions, i.e infiltrate, cavity and consolidation with odd-ratio (OR) of 14, 13, and 3, respectively. In MDR-TB, the only significant lesion is a nodule, with OR of 19.

Conclusion: Nodule is the only type of lesions that distinguish MDR-TB and DS-TB. Infiltrate, cavity and consolidation were the types of chest radiography lesions on DS-TB, meanwhile, a nodule was the only significant lesion for MDR-TB.

KEYWORDS

chest radiography; tuberculosis; DS-TB; MDR-TB

AUTHOR AFFILIATIONS

[1] Departement of Radiology, Temanggung Regional Hospital, Central Java, Indonesia
[2] Departement of Radiology, Persahabatan Hospital, Jakarta, Indonesia
[3] National Institute of Health Research and Development, Indonesian Ministry of Health, Jakarta, Indonesia
[4] Departement of Pulmonology and Respiratory Medicine, Faculty of Medicine Universitas Indonesia, Persahabatan Hospital, Jakarta, Indonesia
* Corresponding author: Department of Pulmonology and Respiratory Medicine, Faculty of Medicine Universitas Indonesia, Persahabatan Hospital, Jalan Persahabatan Raya No. 1, Rawamangun Jakarta 13230, Indonesia; e-mail: fariz.nurwidya@gmail.com

Received: 23 April 2018
Accepted: 22 January 2019
Published online: 1 April 2019

Acta Medica (Hradec Králové) 2019; 62(1): 24–29
https://doi.org/10.14712/18059694.2019.42

List of abbreviations: AFB, acid-fast bacilli; CI, confidence interval; DS-TB, drug-sensitive tuberculosis; GGO, ground glass opacity; HIV, human immunodeficiency virus; MDR-TB, multidrug resistant tuberculosis; MTB, *Mycobacterium tuberculosis*; NTM, Non-Tuberculous Mycobacterium; OR, odds ratio; TB, tuberculosis; WHO, World Health Organization; XDR-TB, extremely drug resistant tuberculosis.

INTRODUCTION

World Health Organization (WHO) predicted an increasing multi-drug resistant tuberculosis (MDR-TB) morbidity and mortality (1, 2, 3). Diagnosis of TB by using sputum culture with MDR-TB susceptibility test takes a long time, therefore WHO developed the GeneXpert method which only takes 2 to 4 hours to diagnose MDR-TB (4). The sensitivity and specificity of GeneXpert and acid-fast bacilli (AFB) were 95.3% vs 60.5% and 86.4% vs 98.5%, respectively (5).

In addition, chest radiography is the only simple, cost-effective, selected, safe, and important imaging modality to detect lesions morphology in the lung especially in pre-clinical stages. In observing TB treatment improvement, a chest x-ray is usually performed at 2 months and 6 months after starting therapy. In TB with the negativity of AFB smear or sputum culture, diagnosis and observation of treatment improvement are based on clinical symptoms and chest radiography findings (6).

There has been no study or data described the comparison of characteristic of drug-sensitive TB (DS-TB) and MDR-TB lesions on chest radiograph in the out-hospital setting. Based on these facts, the problems of this study can be formulated, whether there is a different characteristic of DS-TB lesions of chest radiography compared with AFB smear or sputum culture and GeneXpert-based MDR-TB on the patients of 15 years old or more in order to early detection efforts.

MATERIALS AND METHODS

This is a cross-sectional retrospective study with national and regional coverage. This study was conducted at the National Institute of Health Research and Development, Indonesian Ministry of Health, Jakarta. Data were collected for 3 consecutive days on 16–18 December 2016. Database of national TB prevalence survey 2013–2014 was used. Stratified multi-stage sampling technique was used to populations of 15 years old and above.

Subjects of the study were collected from the secondary data at the Ministry of Health., the Republic of Indonesia. The sample of this study were patients of 15 years old or over with a complaint of coughing of more than 14 days or coughing up blood, who performed chest radiograph study, sputum AFB smear and continued with culture for *Mycobacterium tuberculosis* (MTB) and GeneXpert test, lived in special cluster area at least for one month, excluding individuals living in military barracks, diplomatic mission homes, hospitals, hotels, dormitories, and temporary shelters. The subjects should fulfil the inclusion criteria of patients with MTB chest radiograph, with a final diagnosis of MDR-TB and with the final barcode diagnosis DS-TB.

The exclusion criteria are patients with incomplete medical record data, with chest radiograph indicating other abnormalities of parenchyma, with massive pleural effusion and pneumothorax causing the lung parenchyma could not be assessed. Direct Digital Radiography DICOM (Agva Healthcare, South Carolina, US) was used to perform chest X-ray and the results were read by 3 thoracic radiologists.

The independent variables studied were locations of the lesion on the chest radiograph, whether on the right or left lung. The upper field is an area restricted to lung apex, 2nd anterior costae, and midline projected from procesus spinosus. The medium field is an area restricted from the 2nd to 4th costae and midline projected from processus spinosus. The lower field in an area restricted from the 4th to 6th costae and midline projected from processus spinosus. The type of lesions studied as independent variables were infiltrate, cavity, nodule, mass, consolidation, pleural effusion, pleural thickening (thickening of the pleura), fibrosis and calcification. The dependent variables studied were MDR-TB and DS-TB. MDR-TB is defined as sputum AFB (+/–), culture (+) and GeneXpert (+), meanwhile DS-TB is defined as sputum AFB (+/–), culture (+) and GeneXpert (–). Data collection is done by reviewing the medical record of each patient. The data were analyzed using the Statistical Package for Social Science (SPSS) software program version 21 (IBM Corp, Armonk, NY, USA). Chi-square (x^2) data processing was used for bivariate analysis and logistic regression for multivariate analysis. $P < 0.05$ was considered to be statistically significant.

RESULTS

Participants who met inclusion and exclusion criteria were 147 DS-TB and 11 MDR-TB patients (Tabel 1). Non-Tuberculous Mycobacterium (NTM) patients were included

Tab. 1 Distribution of participant according to characteristics.

Characteristic	DS-TB	MDR-TB
Age group		
15–34	47	6
35–54	58	4
>55	42	1
Sex		
Man	107	9
Woman	40	2
History of tuberculosis treatment		
No	112	3
Yes	35	8

Abbreviations: DS-TB, drug sensitive tuberculosis; MDR-TB, multidrug resistant tuberculosis.

Tab. 2 Association of lesion on chest radiograph and DS-TB.

Variables		DS-TB				P	OR		
		Yes		No					
		F	%	F	%			Lower	Upper
Infiltrate	Present	96	67.6	46	32.4	0.000	13.708	8.666	21.685
	No	51	13.2	335	86.8				
Cavity	Present	41	73.2	15	26.8	0.000	9.438	5.028	17.715
	No	106	22.5	366	77.5				
Nodule < 3 cm	Present	28	60.9	18	39.1	0.000	4.745	2.534	8.885
	No	119	24.7	363	75.3				
Mass	Present	1	11.1	8	88.9	0.249	0.319	0.040	2.576
	No	146	28.1	373	71.9				
Consolidation	Present	55	72.4	21	27.6	0.000	10.248	5.898	17.807
	No	92	20.4	360	79.6				
Pleural effusion	Present	17	68.0	8	32.0	0.000	6.097	2.571	14.462
	No	130	25.8	373	74.2				
Pleural thickening	Present	13	59.1	9	40.9	0.001	4.010	1.676	9.596
	No	134	26.5	372	73.5				
Fibrosis	Present	45	50.0	45	50.0	0.000	3.294	2.061	5.265
	No	102	23.3	336	76.7				
Calcification	Present	14	41.2	20	58.8	0.073	1.900	0.933	3.870
	No	133	26.9	361	73.1				

Abbreviations: DS-TB, drug-sensitive tuberculosis; OR, odd-ratio.

in statistical data calculation, aiming to avoid any bias in the description of lesions characteristic. First, we determined the association of lesion on chest radiograph and DS-TB incidence. As seen in Table 2, infiltrate, cavity, nodule, consolidation, pleural effusion, pleural thickening, and fibrosis were significantly associated with DS-TB incidence.

We then clarified what lesion is predominantly found in DS-TB by performing multivariate analysis (logistic regression). Based on findings in Table 3, there were three types of lesions (infiltrate, cavity, and consolidation) having a *P* value of <0.05. Thus it is concluded that infiltrate, cavities and consolidations features can be used to predict the presence of DS-TB.

Tab. 3 Result of Multivariate analysis of lesions on Chest radiography DS-TB.

Variables	Sig.	OR	95.0% CI for EXP(B)	
			Lower	Upper
Infiltrate	0.000	13.706	7.833	23.982
Cavity	0.006	2.949	1.367	6.364
Nodul	0.375	0.629	0.226	1.751
Mass	0.839	0.788	0.079	7.844
Consolidation	0.000	12.767	5.661	28.796
Pleural effusion	0.150	2.157	0.757	6.143
Pleural thickening	0.717	0.814	0.267	2.478
Fibrosis	0.975	0.989	0.510	1.919
Calcification	0.563	1.359	0.480	3.852

Abbreviations: DS-TB, drug-sensitive tuberculosis; CI, confidence interval; OR, odd-ratio.

Next, we analyze the association of lesion on chest radiograph and MDR-TB incidence. Based on the findings in Table 4, infiltrate, cavity, nodule, and fibrosis were significantly associated with MDR-TB incidence. We also performed multivariate analysis of lesions on chest radiograph in MDR-TB. We found that nodule has P value of <0.05, which mean that nodule can be used to predict the presence of MDR-TB (Table 5).

Finally, we compared the chest radiography characteristics of DS-TB and MDR-TB. A different test is done by chi squre (x^2) test. Based on the analysis in Table 6, nodular lesions have *P* value of <0.05, which suggest that nodule is the only type of lesion that can distinguish MDR-TB and DS-TB.

DISCUSSION

MDR-TB is highly prevalent and studies to reveal the role of radiology imaging in the identification of patients who are suspected to have MDR-TB are under intensive investigation. The diagnosis of TB is established on the basis of clinical history, physical examination, radiology, and bacteriological study. GeneXpert test was used for rapid

Tab. 4 Association of lesions on chest radiograph and MDR-TB.

Variables		MDR-TB				P	OR	C.I 95%	
		Yes		No					
		F	%	F	%			Lower	Upper
Infiltrate	Yes	7	5.0	133	95.0	0.010	5.053	1.456	17.533
	No	4	1.0	384	99.0				
Cavity	Yes	4	7.1	52	92.9	0.021	5.110	1.447	18.041
	No	7	1.5	465	98.5				
Nodule < 3 cm	Yes	5	11.1	40	88.9	0.001	9.938	2.905	33.995
	No	6	1.2	477	98.8				
Mass	Yes	0	0.0	9	100.0	1.000	–	–	–
	No	11	2.1	508	97.9				
Consolidation	Yes	4	5.3	71	94.7	0.057	3.590	1.025	12.576
	No	7	1.5	446	98.5				
Pleural effusion	Yes	1	4.0	24	96.0	0.417	2.054	0.253	16.709
	No	10	2.0	493	98.0				
Pleural thickening	Yes	2	9.5	19	90.5	0.067	5.825	1.177	28.826
	No	9	1.8	498	98.2				
Fibrosis	Yes	5	5.7	83	94.3	0.010	4.357	1.300	14.610
	No	6	1.4	434	98.6				
Calsification	Yes	1	3.1	31	96.9	0.501	1.568	0.194	12.643
	No	10	2.0	486	98.0				

Abbreviations: F, frequency; MDR-TB, multidrug resistant tuberculosis; CI, confidence interval; OR, odd-ratio.

diagnosis of MDR-TB and it is mandatory to perform the drug susceptibility testing of isoniazid and rifampicin. Chest radiography is a simple, cost-effective, selective, safe and important imaging modality in detecting morphology of lung lesions, especially in pre-clinical stage. In addition, the extent of lesions, activity of lesions, pleural involvement and complications such as fungal infection and bronchiectasis can be assessed by using chest radiography.

Tab. 5 Multivariate analysis of lesions on chest radiograph in MDR-TB.

Variables	Sig.	OR	95.0% CI for EXP(B)	
			Lower	Upper
Infiltrate	0.281	2.147	0.536	8.606
Cavity	0.232	2.428	0.566	10.410
Nodule	0.003	18.812	2.627	134.692
Mass	0.999	0.000	0.000	
Consolidation	0.194	0.255	0.032	2.006
Pleural effusion	0.866	1.234	0.107	14.282
Pleural thickening	0.435	2.224	0.299	16.547
Fibrosis	0.149	2.871	0.686	12.016
Calsification	0.589	0.524	0.050	5.483

Abbreviations: MDR-TB, multidrug resistant tuberculosis; CI, confidence interval; OR, odd-ratio.

This study determined the association of lesions with the incidence of DS-TB and MDR-TB. Infiltrates, cavities, nodules, consolidation, pleural effusion, pleural thickening, fibrosis, and calcification are significantly associated with the incidence of DS-TB. Furthermore, the multivariate analysis revealed three lesions (infiltrates, cavities and consolidations) that can be used to predict the presence of DS-TB. In the MDR-TB, the infiltrates, cavities, nodules, and fibrosis, were associated with the incidence of MDR-TB.

According to a study conducted by Zahirifard et al., MDR-TB has more destructive lung features when compared with people with DS-TB (7). The study found that the presence of multiple cavities, nodular lesions, infiltrates and pleural effusions is a major sign of MDR-TB when compared to DS-TB.

Based on the study conducted by Yeom et al., in 2009 in South Korea on radiological features of patients with DS-TB and MDR-TB, it was found that lobular consolidation was more common in patients with DS-TB (8). In addition, the cavity also has a fairly significant prediction value. In general, multiple cavity formations are more common in MDR-TB patients. In addition to the above characteristics, the regression analysis in this study concluded that unilateral parenchymal lesions are more common in people with DS-TB. Yeom et al., also suggested that the level of endemicity of a country and population setting can provide different radiological characteristics so that thorough

Tab. 6 Comparison of characteristic of lesion on chest radiograph in DS-TB with MDR-TB.

Variables		Result				*P* value	OR	C.I 95%	
		MDR-TB		DS-TB					
		F	%	F	%			Lower	Upper
Infiltrate	Yes	7	6.8	96	93.2	1.000	0.930	0.260	3.326
	No	4	7.3	51	92.7				
Cavity	Yes	4	8.9	41	91.1	0.510	1.477	0.411	5.315
	No	7	6.2	106	93.8				
Nodule < 3 cm	Yes	5	15.2	28	84.8	0.038	3.542	1.008	12.438
	No	6	4.8	119	95.2				
Mass	Yes	0	0.0	1	100.0	1.000			
	No	11	7.0	146	93.0				
Consolidation	Yes	4	6.8	55	93.2	1.000	0.956	0.268	3.414
	No	7	7.1	92	92.9				
Pleural effusion	Yes	1	5.6	17	94.4	1.000	0.765	0.092	6.351
	No	10	7.1	130	92.9				
Pleural thickening	Yes	2	13.3	13	86.7	0.280	2.291	0.447	11.744
	No	9	6.3	134	93.7				
Fibrosis	Yes	5	10.0	45	90.0	0.307	1.889	0.548	6.511
	No	6	5.6	102	94.4				
Calsification	Yes	1	6.7	14	93.3	1.000	0.950	0.113	7.979
	No	10	7.0	133	93.0				

Abbreviations: F, frequency; DS-TB, drug sensitive tuberculosis; MDR-TB, multidrug resistant tuberculosis; CI, confidence interval; OR, odd-ratio.

study and analysis of all TB endemic countries is needed to obtain more accurate results.

In 2011, Kim et al., conducted a study to compare CT Scan features in MDR-TB and DS-TB among human immunodeficiency virus (HIV) negative patients (9). In that univariate analysis, it found that bronchiektasis, pulmonary destruction, granuloma calcification, and cavity formation are often found in patients with MDR-TB. The result of the multivariate analysis showed that cavity formation was the only characteristic that differentiated MDR-TB and DS-TB.

We have previously described that there was no significant difference in morphology and lesion location on the chest radiograph of both pulmonary tuberculosis with negative AFB smear and positive culture and negative AFB smear and negative culture (10). Pulmonary TB with negative AFB smear and positive culture lung tend to have more extent lesions. Chest radiograph of 67 pulmonary TB patients with negative AFB smear and positive culture and 89 pulmonary TB patients with negative AFB smear and negative culture patients mostly showed infiltrate (41.0% vs 32.0%) followed by cavities (14.2% vs 12.2 %), consolidation (12.4% vs 14.2%) and pleural effusion (0.33% vs 0.35%).

In this study, a different test was performed by Chi-square (x^2) test on the comparison of DS-TB and MDR-TB characteristics. Based on the analysis, nodules is the only the type of lesion that was significantly typical for DS-TB with an OR value of 3.5 compared to MDR-TB. This finding is consistent with our previous study and the study by Cha et al., who examined the radiographic features of patients with MDR-TB, XDR TB and compared it with DS-TB (11, 12). They found that the features of nodules and ground glass opacity (GGO) were more prevalent in TB patients who were still sensitive to anti TB drugs (DS-TB). While the radiological features in patients with MDR-TB and XDR TB are multiple cavities, nodules, and bronchial dilatation. Radiologic features of patients with MDR-TB and XDR TB were not significantly different. The study also discovered that patients with MDR-TB and XDR TB were younger than the DS-TB patients. Further study was necessary to see if there were multiple nodules and cavities and bronchial dilatation in young TB patients.

The study is limited with the fact that the MDR-TB cases were only consist of eleven cases. This may implicate in the limited conclusion to a broader population. Other limitation is that several subjects with non-tuberculosis mycobacterium (NTM) were included in the analysis together with TB patients.

CONCLUSION

As a conclusion, nodules are the only characteristic lesions in chest radiographs that distinguish between MDR-TB and DS-TB. The lesions that are significantly associated with the DS-TB were infiltrates, cavities, nodules, consolidations, pleural effusions, pleural thickening, fibrosis and calcification, and the OR of infiltrates, consolidation,

and cavity were 14, 13 and 3, respectively. The lesions that are significantly associated with MDR-TB were infiltrates, cavities, nodules and fibrosis, and the OR of the nodule was 19 in MDR-TB.

REFERENCES

1. Word Health Organization, 2014. Global Tuberculosis Report 2014. Geneva: Word Health Organization.
2. Word Health Organization, 2009. A brief history of tuberculosis control in Indonesia. Geneva Word Health Organization
3. Word Health Organization, 2017. Global Tuberculosis Report 2017. Geneva: Word Health Organization.
4. World Health Organization, 2008. Management of MDR-TB: A field guide. Geneva: World Health Organization.
5. Pinyopornpanish K, Chaiwarith R, Pantip C, et al. Comparison of Xpert MTB/RIF Assay and the Conventional Sputum Microscopy in Detecting Mycobacterium tuberculosis in Northern Thailand. Tuberc Res Treat 2015; 2015: 571782.
6. Icksan AG, Luhur R. 2008. Thoracic Radiology of Pulmonary Tuberculosis, the First Edition [Radiologi toraks TB paru, Edisi Pertama]. Jakarta. CV Sagung Seto.
7. Zahirifard S, Amiri MV, Karam B, et al. The Radiological Spectrum of Pulmonary Multidrug-Resistant Tuberculosis In HIV-Negative Patients. Iran J Radiol 2003; 1: 161–6.
8. Yeom JA, Jeong YJ, Jeon D, et al. Imaging findings of primary multi drugresistant tuberculosis: A comparison of findings of drug-sensitive tuberculosis. J Comput Assist Tomogr 2009; 33: 956–60.
9. Kim HC, Goo JM, Park SH, Park CM, Kim TG. Multidrug-resistant TB versus Drug-sensitive TB in human immunodeficiency virus-negative patoient: computed tomgraphy features. J Comput Assist Tomogra 2004; 28: 366-71.
10. Icksan AG, Maryastuti M. Characteristics of chest X-Ray lesion in smear-negative TB patient with culture-positive vs culture-negative in the Persahabatan Hospital, Jakarta. Bul Ilmiah Radiol 2012; 2: 80–90. [Indonesian Society of Radiology chapter Yogyakarta and Department of Radiology, University of Gajah Mada Faculty of Medicine, Yogyakarta].
11. Icksan AG, Napitupulu MRS, Nawas MA, Nurwidya F. Chest X-ray Findings Comparison Between Multi-drug-resistant Tuberculosis and Drug-sensitive Tuberculosis. J Nat Sci Biol Med 2018; 9: 42–5.
12. Cha J, Lee HY, Lee KS, et al. Radiological Findings of Extensively Drug-Resistant Pulmonary Tuberculosis in Non-AIDS Adults: Comparisons with Findings of Multidrug-Resistant and Drug-Sensitive Tuberculosis. Korean J Radiol 2009; 10: 207–16.

Cytotoxic Effects of Pistacia Atlantica (Baneh) Fruit Extract on Human KB Cancer Cell Line

Zohreh Jaafari-Ashkvandi[1], Saeed Yousefi Shirazi[2], Somayeh Rezaeifard[3], Azadeh Hamedi[4], Nasrollah Erfani[5,*]

ABSTRACT

Plants with anticancer properties are considered as cancer preventive and treatment sources, due to their some biological effects. Apoptosis induction and anti-proliferative effects of Baneh extract on various cancer cell lines have been reported. Hence, this study was designed to evaluate the cytotoxic effects of this fruit on KB and human gingival fibroblast cell lines (HGF). KB and HGF cells were treated with various concentrations of ethanolic Baneh extract and cisplatin as positive control. Cytotoxic activity and apoptosis induction were investigated using WST-1 and Annexin V assays. Data were analyzed using ANOVA and student's t-tests. IC_{50} after 24 and 48 hours treatment were respectively 2.6 and 1 mg/mL for KB cell line, and 1.5 and 1.6 mg/mL for HGF cell. During 48 hours Baneh extract induced apoptosis without significant necrosis, in a time- and dose-dependent manner. The induction of apoptosis in KB cells was significantly higher than HGF. It seems that ethanolic extract of Baneh contains compounds that can suppress KB cell growth through the induction of apoptosis. Within 48 hours, less cytotoxic effects were observed on normal fibroblast cells; therefore, it might be a potential anticancer agent.

KEYWORDS

pistacia; Baneh; squamous cell carcinoma; cytotoxicity; apoptosis; fibroblast; cell line

AUTHOR AFFILIATIONS

[1] Department of Oral & Maxillofacial pathology, School of Dentistry, Shiraz University of Medical Sciences, Shiraz, Iran
[2] School of Dentistry, Shiraz University of Medical Sciences, Shiraz, Iran
[3] Shiraz Institute for Cancer Research, School of Medicine, Shiraz University of Medical Sciences, Shiraz, Iran
[4] Department of Pharmacognosy, School of Pharmacy, Shiraz University of Medical Sciences, Shiraz, Iran
[5] Department of Immunology and Shiraz Institute for Cancer Researches, School of Medicine, Shiraz University of Medical Sciences, Shiraz, Iran
* Corresponding author: Department of Immunology and Shiraz Institute for Cancer Researches, School of Medicine, Shiraz University of Medical Sciences, Shiraz, Iran; e-mail: erfanin@sums.ac.ir

Received: 25 September 2018
Accepted: 26 January 2019
Published online: 1 April 2019

Acta Medica (Hradec Králové) 2019; 62(1): 30–34
https://doi.org/10.14712/18059694.2019.43

INTRODUCTION

Squamous cell carcinoma (SCC) is the most common head and neck cancer. Despite advances in the medical research and therapies, 5-years survival rate is not favorable, yet. Surgery is the first therapeutic management and many patients require adjuvant radio-and chemotherapy (1). These anticancer approaches induce many non-specific involuntary cellular effects, cell death, tissue toxicity and several complications in patients (2). Today, there is an ever growing interest toward herbal medicine to treat cancer, due to low tissue toxicity and specific toxic effects on cancer cells (3). Herbs can act as alternative and complementary medicine. Natural compounds can reduce inflammation and counteract chemotherapy resistant (4).

Pistacia atlantica (*P. atlantica*) is a member of Anacardiaceae family, which grows from the Mediterranean basin to central Asia. *P. atlantica* subsp. *krudica*, known as Baneh is distributed in west mountainous region of Iran. The unripe fruits and the seeds of the plant are widely used as edible fruit, as nuts or in foods. The oleo-gum resin of the plant as well as its fruits and seeds are used in Persian Traditional Medicine (PTM) for treating digestive, hepatic, skin and kidney diseases (5, 6). Recently, different parts of the plant has exhibited some biological effects, such as anti-arteriosclerosis, , anti-inflammatory, antifungal and antimicrobial effects as well as cytotoxic properties in various human cancer cell lines (7). The main goal of anticancer agents is to induce tumoral cell death and control cell cycle (8). Previous studies on the cytotoxic effects of *P. atlantica* have shown the induction of apoptosis in prostate, colon, lung and breast cancer cell lines (9–11). These effects mostly are contributed to neutralizing free radicals, metal chelating and regulating of enzymatic activity due to presence of some component, such as flavonoids and polyphenols in this plant (12).

Polyphenolic components of the plant could also regulate the cell cycle progression through regulating genes that are related to cell proliferation and apoptosis (13). *P. atlantica* extract down-regulated cyclin A protein and S-phase of cell cycle in human colon carcinoma cell line (10). Also, it has induced G0/G1 arrest and has decreased the expression of cyclin D1 and cyclin dependent kinase 4 (CDK4) in breast cancer cell line (11).

Due to the potential cytotoxic effects of Baneh extract on several human cancer cell lines, this study aimed to evaluate its cytotoxic effect on KB (subline of HeLa cells with oral cancer properties) and normal human fibroblast cell line of the oral cavity. KB cells initially isolated from an oral SCC, however, they have been reported to be contaminated with HeLa cells and are considered as a subline of the these cells (14).

METHODS AND MATERIAL

PLANT MATERIALS

Fresh fruit of Baneh (*P. atlantica* subsp. *krudica*) was collected in Fars province (April, 2016) and was authenticated by a pharmcognosist at Shiraz University of Medical Sciences. The fruits were grinded and then macerated in 70% ethanol in a dark and closed glass container (3 × 48 hours). The collected hydroalcoholic extract was concentrated by a rotary evaporator at 40 °C and stored at –20 °C.

CELL LINE AND CULTURE

KB cells and human gingival fibroblast cell line (HGF) were purchased from the Pasture Institute cell bank in Tehran, Iran. The cells were cultured in RPMI-1640 and DMEM (Biosera-UK) medium supplemented with 10% fetal calf serum, 1% penicillin and 1% streptomycin (Biosera-UK), respectively. The cell cultures were grown in a 5% CO_2 incubator at 37 °C.

CYTOTOXICITY ASSAY

Cell viability of both cell lines was assessed by WST-1 test. The cells were cultured in 96 well, flat-bottoms microplates with a final volume of 200 µL/well. Total of 10,000 cell/well were incubated in 5% CO_2 at 37 °C for 24 hours. Then, Baneh extract with 0, 0.25, 0.5, 0.75, 1 mg/mL dilutions and also cisplatin with 0, 20, 40, 80 µg/mL dilutions (as positive control) were added and incubated at 37 °C, 5% CO_2. After 24 and 48 hours treatment, 10 µL WST-1 solution was applied to the wells and incubated for 4 hours, again. Finally, the wells were shaken for 1 minute and optical density (OD) was measured by spectrophotometry at 480 nm using multimode microplate reader. The culture medium background was subtracted from the results and cytotoxicity percentage was calculated by the following formula: (OD of treated cells/OD of control cells) × 100 – 100.

Then, IC_{50} values – the concentration that inhabits 50% cell growt – were obtained by curve expert software, version 13, in plant extract and control groups. Each experiment was performed triplicate and the results were presented as mean ±SD.

ANNEXIN V/7AAD APOPTOSIS ASSAY

KB and HGF cells were treated with IC_{50}, ½ IC_{50} and 2 × IC_{50} concentrations of Baneh extract for 48 hours. The treated and untreated (control) cells were trypsinized and stained with Annexin V/7AAD (Ann V/7A) kit (BD, USA) to detect apoptotic and necrotic cells. The cells were detected by FACS Calibur flow cytometr (BD Biosciences, USA) and were analyzed using flow Jo software package. According to the manufacture's instruction, data were classified as: viable cells when the stained cells were: Ann (–), 7A (–), early apoptosis: Ann (+), 7A (–), Late apoptosis: Ann (+), 7A (+) and necrotic: Ann V (–), 7A (+). Each analysis was performed 3 times and the means were reported.

Data analyzed by SPSS, version 15 using ANOVA and Mann-Whitney tests.

RESULTS

CELL VIABILITY ASSAY

Cell viability was assessed by WST-1 at 24–48 hours. IC_{50} values for KB and HGF cells after treatment with Baneh extract and cisplatin are shown in Table1. Baneh extract

showed growth inhibition in a dose-and time-dependent manner in KB cells. In HGF cells, the more potent cytotoxic effect was found in 24 hours; however, after 48 hours IC_{50} was slightly elevated. Similar results were found in cells treated with cisplatin.

Tab. 1 Cytotoxic effect of Baneh extract and cisplatin after 24 and 48 hours on KB and HGF cells using WST-1 test.

Agent	IC_{50} KB		IC_{50} HGF	
	24 h	48 h	24 h	48 h
Baneh extract (mg/mL)	2.6 ± 0.04	1.0 ± 0.02	1.5 ± 0.05	1.6 ± 0.03
Cisplatin (µg/mL)	62 ± 2.1	14.6 ± 1.8	154.1 ± 3	193 ± 3.5

APOPTOSIS INDUCTION

Apoptotic and necrotic KB and HGF cells were detected by Ann V/7A staining assay using flow cytometry after 48 hours. The profile of cell distribution is shown in Figures 1 and 2. The percentage of viable, apoptotic and necrotic cells are found in Table 2. Flow cytometric analysis of apoptosis in KB cell line after 48 hours incubation with different concentration of Baneh extract is illustrated in Figure 3. According to the results, in KB cells a significant (>60%) early apoptosis was induced after 48 hours with 1 mg/mL concentration. Also, there was no significant percentage of necrotic cells after 48 hours of treatment. HGF cells showed about 10% apoptosis during that time in IC_{50} concentration (Figure 4). ANOVA analysis revealed significant differences between the treated and untreated KB cells in the percentage of live, apoptotic and necrotic cells. Post-hoc Dunn analysis showed that the difference was significant between the percentages of the live and the early apoptotic populations, as well as between the early and the late apoptotic populations. Furthermore, ANOVA and Dunn analysis revealed this pattern to be repeated in treated and untreated HGF cells; however, there was no significant difference in the percentages of the late apoptotic and necrotic cells in this cell line (Table 2).

Tab. 2 The percentage of live, apoptotic and necrotic cells in all study cell lines.

	Concentration	KB	HGF
Live cell	IC_{50}	12.92 ± 0.31*	88.73 ± 1.00*
	Ctrl (0)	91.45 ± 0.20	95.50 ± 1.22
Early apoptosis	IC_{50}	74.00 ± 0.10*	12.44 ± 1.00*
	Ctrl	6.13 ± 0.05	4.32 ± 0.31
Late apoptpsis	IC_{50}	12.62 ± 0.34*	1.11 ± 0.01
	Ctrl	2.33 ± 0.18	0.20 ± 0.03
Necrosis	IC_{50}	0.49 ± 0.11	0.18 ± 0.05
	Ctrl	0.17 ± 0.05	0.05 ± 0.00

* Significant when compare to control (using Dunn post-hoc test).

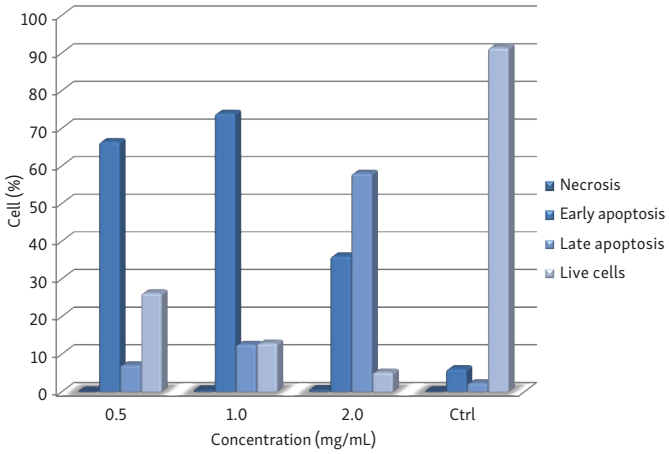

Fig. 1 Annexin V/PI apoptotic assay on Baneh extract treated KB cells after 48 hours.

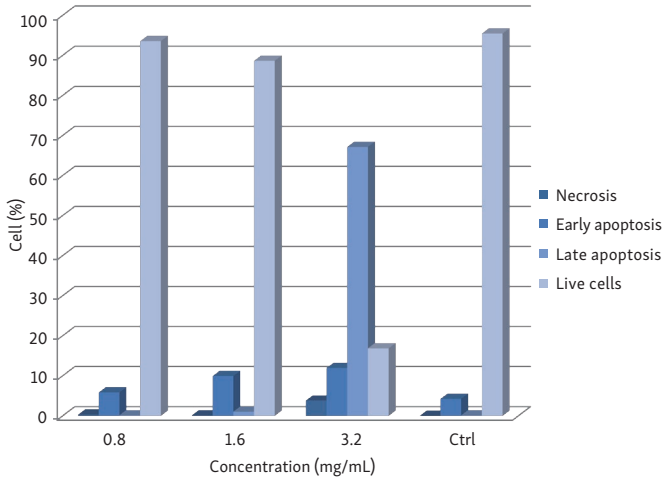

Fig. 2 Annexin V/PI apoptotic assay on Baneh extract treated HGF cells after 48 hours.

DISCUSSION

Insufficient apoptosis is a feature of cancer cells. The regulation of apoptosis is a promising target for many anti-cancer drugs (8). Recently, many herbal compounds are recognized with cytotoxic effects on various cancer cells, which can be used as lead compounds for developing new anticancer agents. Natural compounds exert chemotoxic effects via the induction of apoptotic pathways (15). In the present study, the cytotoxic effects of Baneh hydroalcoholic extract on KB and HGF cells were assessed by evaluating cell viability and apoptosis rate. The hydroalcoholic extract is enriched with bioactive polyphenolic compounds (16).

The results showed that Baneh extract exert cytotoxic effects on both cell lines, but it was more pronounced in KB cells after 48 hours. However, this cytotoxic effect was not very potent, especially on HGF cells. Extract IC_{50} values demonstrated that the plant could have cytotoxic compounds and these values could be a result of the additive effect of different compounds in extract. Flow cytometry assay after 48 hours defined that Baneh extract induced apoptosis without significant induction of necrosis. Apoptosis is a well-controlled cell death mechanism for removal

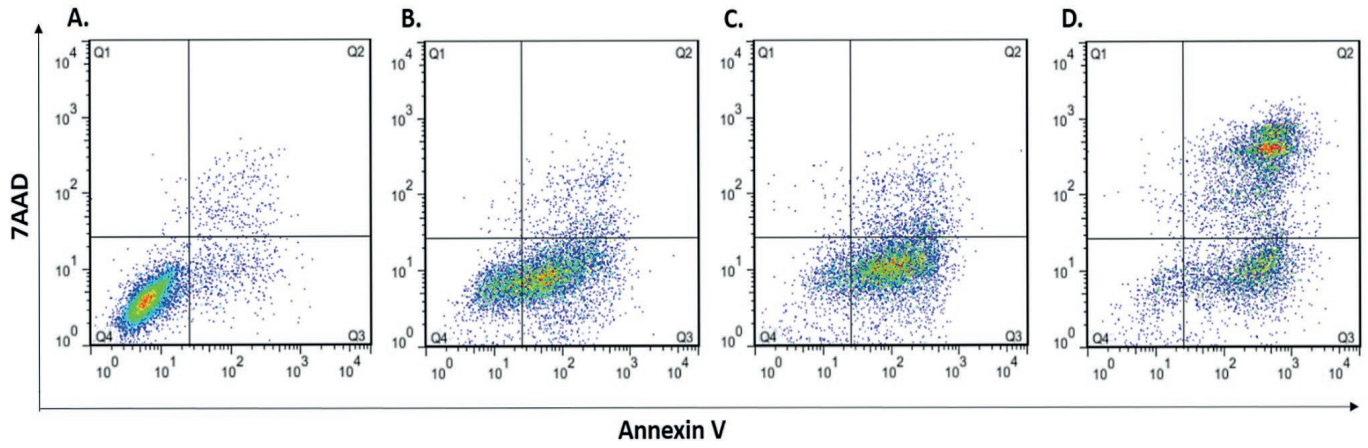

Fig. 3 Flow cytometric analysis of apoptosis in KB cell line after 48 hours treatment with different concentration of Baneh extract; A: untreated cells (control), B: 0.5, C: 1 (IC_{50}), D: 2 mg/mL concentrations.

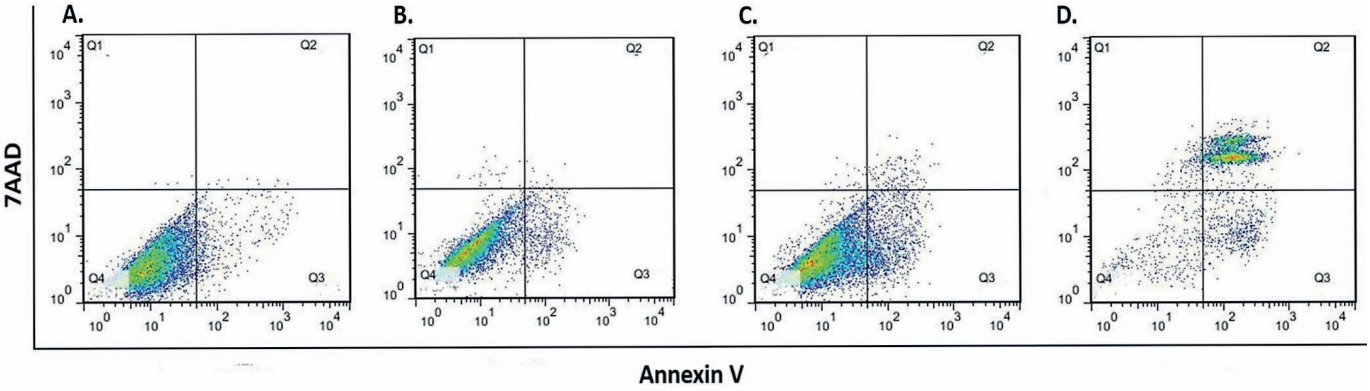

Fig. 4 Flow cytometric analysis of apoptosis in HGF cell line after 48 hours treatment with different concentration of Baneh extract; A: untreated cells (control), B: 0.8, C: 1.6 (IC_{50}), D: 3.2 mg/mL concentrations.

of damaged cells. There are two apoptotic pathways: extrinsic pathway, which is activated via membrane death receptors and intrinsic pathway, which is activated by alteration in mitochondrial membrane; both pathways result in activation of caspases. Insufficient apoptosis plays a crucial role in cancer development (13). Increased apoptosis and cell cycle arrest have been observed in some cancer cell lines in response to various extracts of Baneh. Rezaei et al. stated that treatment of TD47 cells (human breast cancer cell line) for 48 hours, entailed cell cycle arrest via downregulation of cyclin D1 and CDK4. Also, they found that apoptosis was increased to 30% in treated cells, which was more powerful than doxorubicin (11, 15).

In another study, they found that pericarp polyphenolic-rich extract of Baneh induced apoptosis and inhibited cell cycle progression (via delay in S-phase) in human colon carcinoma cells (HT29)(10). Amiri et al. observed apoptosis induction in prostate cancer cell line (PC3) after treatment with ethanolic Baneh skin extract (9).

Some studies reported that plants of Anacardiaceae family could induce apoptosis via different mechanisms. The leaves of *Lithraea molleoides* activated P53-independent apoptosis in hepatocellular carcinoma cell lines (17). Also, poly (ADP-ribose) polymerase (PARP) cleavage and caspase activation were induced by *Semecarpus anacardium* nut oil in leukemia and breast cancer cell lines (12, 18). *P. lentiscus* extract lead to cleavage of procaspase-3 and activation of caspase in oral cancer cells (19). Baneh extract caused a time-dependent activation of caspase 3 and PARP cleavage in TD47 cells (15).

Polyphenolic compounds including flavonoids and non-flavonoids were found in all parts of Baneh nut. Many polyphenols could act as potent anti-cancer agents due to their antioxidant properties (9, 20). Also, polyphenols have induced activation of apoptotic transcription factor and enhanced apoptosis in many cancer cells (12). Flavonoids arrested different cell cycle phases and reduced tumor growth in animal models (21).

According to the results of cell viability assay in 24 and 48 hours, Baneh extract induced more powerful cytotoxic effects on HGF cells in 24 hours; however, IC_{50} was increased after 48 hours of treatment. This pattern was also found in the study of ethanolic extract of Baneh skin on mouse fibroblast cell line (L929) in comparison with PC3 cells. However, the researchers did not find a significant difference in cytotoxic effects of Baneh extract on L929 cell line after 48 and 72 hours (9). It seems that normal fibroblasts could become resistance to cytotoxic effects of the plant compounds over time. Furthermore, HGF cells are mesenchymal cells; hence, it is possible to react with herbal compounds in a different manner in comparison with neoplastic epithelial cells.

There are two cell death mechanisms that can be induced by cytotoxic agents and drugs; apoptosis and necrosis. In the present study, Baneh extract increased apoptosis without significant necrosis. Necrosis can stimulate pro-inflammatory response that can lead to infiltration of immune cells in the tumor site. This process result in increasing effects of cytotoxic drugs, but also an inflammatory response can activate mitogens or cytokines and promote cell growth, migration and tumor metastasis (22, 23). Many anticancer agents, such as cisplatin, taxol and 5-fluorouracil (5-FU), which are routinely used for head and neck cancers, act via induction of both mechanisms (24). Furthermore; a few studies have shown that necrosis might be a preferred mechanism for anticancer treatments (25). Due to dual function of anticancer agents it is necessary to evaluate usefulness as well as side effects of any potential anticancer agent through *in vivo* studies. Further studies are expected to search for the exact mechanism of tumoral cell death, as well as monitoring the effect of Baneh extract on non-tumoral host tissues as well as emphasizing the clinically relevant action of this compound.

CONCLUSION

The study findings indicated that Baneh extract was able to induce apoptosis, without significant increase of necrosis in KB cells. During 48 hours, cytotoxic effect was more pronounced in KB cells rather than HGF. Based on the results, Baneh extract may contain metabolites, which could be considered as anticancer agents, however furthers studies are suggested to determine their structures and the possible mechanisms of action.

ACKNOWLEDGEMENTS

This manuscript is based on the undergraduate thesis of S. Yousefi Shirazi. The authors are grateful to Dr. M. Vosoughi at Dental Research Development Center of Shiraz Dental School. This research program was funded by Vice-chancellery of Shiraz University of Medical Sciences (Grant #8895148). The authors wish to thank Mr. H. Argasi at the Research Consultation Center (RCC) of Shiraz University of Medical Sciences for his invaluable assistance in editing this manuscript.

REFERENCE

1. Mosel DD, Bauer RL, Lynch DP, Hwang ST. Oral complications in the treatment of cancer patients. Oral Dis 2011 Sep; 17(6): 550–9.
2. Astolfi L, Ghiselli S, Guaran V, et al. Correlation of adverse effects of cisplatin administration in patients affected by solid tumours: a retrospective evaluation. Oncol Rep 2013 Apr; 29(4): 1285–92.
3. Greenwell M, Rahman PK. Medicinal Plants: Their Use in Anticancer Treatment. Int J Pharm Sci Res 2015 Oct 1; 6(10): 4103–12.
4. Pistollato F, Calderón Iglesias R, et al. The use of natural compounds for the targeting and chemoprevention of ovarian cancer. Cancer Letters 2017; 411: 191–200.
5. Bozorgi M, Memariani Z, Mobli M, Salehi Surmaghi MH, Shams-Ardekani MR, Rahimi R. Five *Pistacia* species (*P. vera*, *P. atlantica*, *P. terebinthus*, *P. khinjuk*, and *P. lentiscus*): a review of their traditional uses, phytochemistry, and pharmacology. The Scientific World Journal 2013; 2013: 219815.
6. Avicenna. The Canon. Tehran, Iran: Soroush Press; 2008.
7. Peksel A. Antioxidative properties of decoction of *Pistacia atlantica* Desf. leaves 2008. 681–93 p.
8. Pfeffer CM, Singh ATK. Apoptosis: A Target for Anticancer Therapy. Int J Mol Sci 2018 Feb 2; 19(2): 448.
9. Amiri M, Kazerouni F, Namaki S, et al. Cytotoxic Effects of the Ethanol Bane Skin Extract in Human Prostate Cancer Pc3 Cells. Iran J Cancer Prev 2016 Apr; 9(2): e4755.
10. Rezaei PF, Fouladdel S, Hassani S, et al. Induction of apoptosis and cell cycle arrest by pericarp polyphenol-rich extract of Baneh in human colon carcinoma HT29 cells. Food and Chemical Toxicology 2012; 50(3): 1054–9.
11. Rezaei PF, Fouladdel S, Ghaffari SM, Amin G, Azizi E. Induction of G1 cell cycle arrest and cyclin D1 down-regulation in response to pericarp extract of Baneh in human breast cancer T47D cells. DARU Journal of Pharmaceutical Sciences 2012; 20(1): 1.
12. Mathivadhani P, Shanthi P, Sachdanandam P. Apoptotic effect of *Semecarpus anacardium* nut extract on T47D breast cancer cell line. Cell Biology International 2007; 31(10): 1198–206.
13. Keating E, Martel F. Antimetabolic Effects of Polyphenols in Breast Cancer Cells: Focus on Glucose Uptake and Metabolism. Front Nutr 2018; 5: 25.
14. Jiang L, Zeng X, Wang Z, Chen Q. Cell line cross-con-tamination:KB is not an oral squamous cell carcinoma cell line. Eur J Oral Sci 2009; 117: 90–1.
15. Rezaei PF, Fouladdel S, Cristofanon S, Ghaffari S, Amin G, Azizi E. Comparative cellular and molecular analysis of cytotoxicity and apoptosis induction by doxorubicin and Baneh in human breast cancer T47D cells. Cytotechnology 2011; 63(5): 503–12.
16. Suh SS, Kim SM, Kim JE, et al. Anticancer activities of ethanol extract from the Antarctic freshwater microalga, Botryidiopsidaceae sp. BMC Complementary and Alternative Medicine 2017 Dec 1; 17(1): 509.
17. Barbini L, Lopez P, Ruffa J, et al. Induction of apoptosis on human hepatocarcinoma cell lines by an alkyl resorcinol isolated from *Lithraea molleoides*. World Journal of Gastroenterology 2006 Oct 7; 12(37): 5959–63.
18. Chakraborty S, Roy M, Taraphdar AK, Bhattacharya RK. Cytotoxic effect of root extract of Tiliacora racemosa and oil of *Semecarpus anacardium* nut in human tumour cells. Phytotherapy research: PTR 2004 Aug; 18(8): 595–600.
19. Li S, Cha I-H, Nam W. Chios mastic gum extracts as a potent antitumor agent that inhibits growth and induces apoptosis of oral cancer cells. Asian Pac J Cancer Prev 2011; 12(7): 1877–80.
20. Hatamnia AA, Abbaspour N, Darvishzadeh R. Antioxidant activity and phenolic profile of different parts of Bene (*Pistacia atlantica* subsp. *kurdica*) fruits. Food Chemistry 2014; 145: 306–11.
21. Sak K. Cytotoxicity of dietary flavonoids on different human cancer types. Pharmacognosy Reviews 2014 Jul; 8(16): 122–46.
22. Liu X, Yang W, Guan Z, et al. There are only four basic modes of cell death, although there are many ad-hoc variants adapted to different situations. Cell and Bioscience 2018; 8: 6.
23. Ricci MS, Zong WX. Chemotherapeutic approaches for targeting cell death pathways. The Oncologist. 2006 Apr; 11(4): 342–57.
24. Elias ST, Borges GA, Rego DF, et al. Combined paclitaxel, cisplatin and fluorouracil therapy enhances ionizing radiation effects, inhibits migration and induces G0/G1 cell cycle arrest and apoptosis in oral carcinoma cell lines. Oncology Letters 2015 Sep; 10(3): 1721–7.
25. Zhang J, Lou X, Jin L, et al. Necrosis, and then stress induced necrosis-like cell death, but not apoptosis, should be the preferred cell death mode for chemotherapy: clearance of a few misconceptions. Oncoscience 2014; 1(6): 407–22.

Actinomycotic Endomyometritis Associated with a Long-Term Use of Intrauterine Device Lasting for 42 Years

Vladimír Bartoš[1,*], Jana Doboszová[1], Martin Sudek[2]

ABSTRACT
In women, pelvic actinomycosis is closely associated with prolonged use of the intrauterine devices (IUD). A 70-year old female presented with intermittent blood-stained vaginal discharge. An analysis of her history revealed, she was inserted with an IUD 42 years ago, but it has remained in situ untill now. Curettage of the uterus was done, but an IUD was firmly attached inside the cavity and there was not able to remove it. A biopsy material consisted of the large round and oval granules of filamentous and mycelium-like microorganisms. They showed strong positivity with Periodic acid–Schiff stain and Gömöri methenamine silver stain. Histopathology was consisted with uterine actinomycosis. A total abdominal hysterectomy with bilateral adnexectomy was performed. The uterus contained a retained plastic IUD. Microscopic investigation revealed a diffuse chronic active endomyometritis with sporadic Actinomycetes colonies. Wearing an IUD continuously for very long periods of time can lead to actinomycotic infection, which may manifest for many years after its application. All IUD users have to keep in mind regular gynecological check-ups to avoid the complications of a retained and "forgotten" IUD.

KEYWORDS
actinomycosis; endomyometritis; intrauterine device

AUTHOR AFFILIATIONS
[1] Department of Pathology, Faculty Hospital in Žilina, Slovakia
[2] Department of Gynecology and Obstetrics, Faculty Hospital in Žilina, Slovakia
* Corresponding author: Faculty Hospital in Žilina, Vojtecha Spanyola 43, 012 07, Žilina, Slovakia; e-mail: vladim.bartos@gmail.com

Received: 2 October 2018
Accepted: 9 January 2019
Published online: 1 April 2019

Acta Medica (Hradec Králové) 2019; 62(1): 35–38
https://doi.org/10.14712/18059694.2019.44

INTRODUCTION

Actinomycosis is a chronic suppurative disease caused by Actinomyces species. They represent Gram-positive, anaerobic or microaerophilic bacteria with a tendency to form branching filaments that fragment into the rods (1, 2). They are commensals normally encountered in the oral cavity, gastrointestinal tract, and female genital tract (1, 2). Under normal circumstances, Actinomycetes are unable to cross the mucosal barrier and cause disease. The main predisposing factor for acquiring an infection is an irritation of the mucosa by trauma or foreign bodies, chronic inflammatory disease, and immunosuppression (1, 2). These pathologic conditions allow bacterial entry into the deep tissue through damaged mucosal barrier (1). Actinomycosis exhibits certain specific clinicopathologic characteristics. A densely fibrotic foci spreading in the connective tissue is one of the features. Advanced lesions are accompanied by abscesses formation, which may lead to the development of sinuses and fistulas to adjacent organ structures (1). Histologically, actinomycosis is characterized by the finding of "sulfur granules", which are composed of the bacterial elements and tissue debris. In hematoxylin-eosin staining, "sulfur granules" are identified as round or oval basophilic masses with a radiating fringe of club-shaped configurations (Splendore-Hoeppli phenomenon) (1). The three main clinical forms of actinomycosis include cervicofacial, thoracic, and abdominopelvic. The last form accounts for approximately 20% of the cases (1). In women, pelvic actinomycosis is closely associated with prolonged use of the intrauterine devices (IUD) (1, 2). Herein, we present a unique case of endometrial actinomycosis associated with long-term insertion of an IUD in elderly woman.

CASE PRESENTATION

A 70-year old female who had been postmenopausal for 18 years, visited the Department of Gynecology (July, 2018) with intermittent vaginal discharge. It was brawnish in color and sometimes contained blood. The patient did not complain of pelvic pain nor had a higher body temperature. She had three spontaneous deliveries, the last one being 43 years previously (1975). No spontaneous abortion or medical interruption of pregnancy were recorded. A retrospective analysis of her history revealed that after the third birth, she was inserted (1976) with an IUD, that has remained in the uterus untill now. At present, she has been treated for diabetes mellitus type 2 with disease-related complications.

Per speculum and per vaginal examination did not show any pathologic lesion, that could be a source of discharge. Transvaginal ultrasonography (TVU) revealed a slightly enlarged uterine cavity filled with mixed, hyperechogenic and hypoechogenic masses. An IUD left in situ was clearly identify. The presumptive clinical diagnosis was an endometrial hyperplasia. The other findings of the TVU examination were within normal limits. Under general anesthesia, a curretage of the uterine cavity was done and a tissue specimen was sent for histopathology.

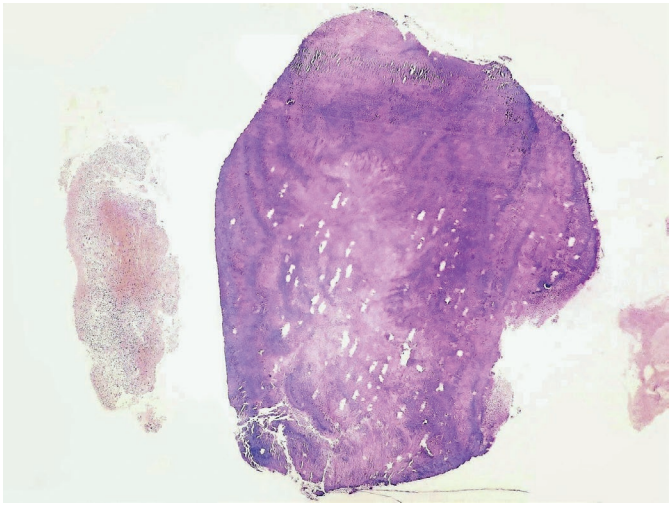

Fig. 1 High-power view of the basophilic masses of Actinomycetes (hematoxylin & eozin, ×40).

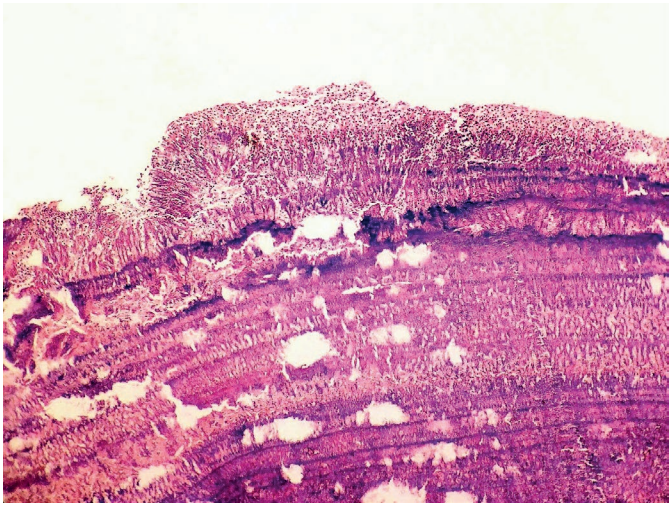

Fig. 2 Periodic acid–Schiff (PAS) stain of Actinomyces colonies. A narow rim of discrete leukocyte cellulisation at the periphery is visible (×100).

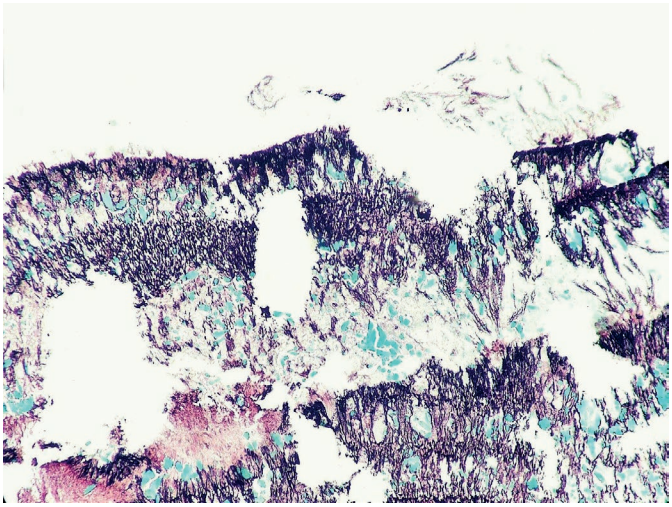

Fig. 3 Gömöri methenamine silver stain highlights abundant mycelia-like structures (×100).

However, an IUD was firmly attached inside the uterus and there was not able to remove it. Microscopically, a biopsy material consisted of the large (up to 5 mm in diameter) round and oval granules of basophilic microorganisms (Fig. 1). At the periphery, they were focally surrounded by thin layer of acute inflamatory infiltration. Splendore-Hoeppli phenomenon was sometimes seen. A high magnification revealed, these colonies were composed of branched filamentous and mycelium-like microorganisms situated in an amorphic matrix. They showed strong positivity with Periodic acid–Schiff (PAS) stain (Fig. 2) and Gömöri methenamine silver stain (Fig. 3). The rest of the biopsy specimen included necrotic inflamatory debris, fragments of heavily inflamed endometrium and blood content. Histopathology was consisted with uterine actinomycosis associated with prolonged use of IUD.

After receiving a biopsy report, the patient was consulted with the specialists to decide the further steps. Considering her age and particularly an inability to extract an IUD from the uterus, a total abdominal hysterectomy with bilateral adnexectomy was done a few weeks later. Grossly, the uterus measured 9 × 5 × 3 cm and contained retained plastic IUD inside the cavity (Fig. 4). An adjacent corporal endometrium appeared thin and hemorrhagic without any marked pathologic foci. Microscopic investigation of the samples revealed a finding of diffuse chronic active endomyometritis. Endometrium was atrophic and massively infiltrated by lymphocytes, plasma cells and leucocytes (Fig. 5), which affected an adjacent myometrium as well. In some areas, endometrium was totally replaced by nonspecific inflammatory granulation tissue. Only in a single excision, the colonies of actinomycotic microorganisms were seen on the surface of almost entirely lost endometrium (Fig. 6). Both ovaries and fallopian tubes were normal without any signs of infection. The postoperative period was uneventful, the patient was administered with oral antibiotic therapy (Bitamon), and she was discharged from the hospital four days after surgery.

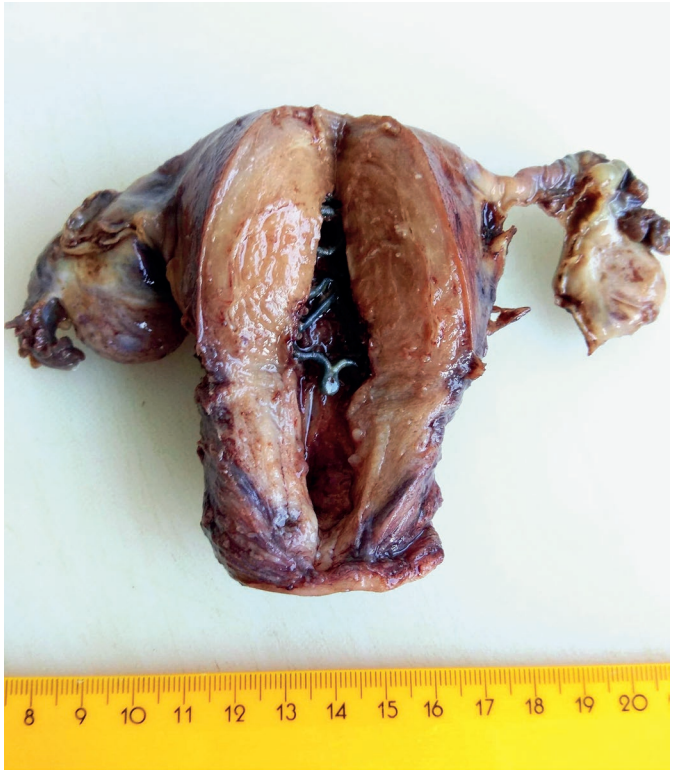

Fig. 4 Uterus with adnexa after hysterectomy (post fixation in formalin). An IUD left in situ is seen inside the cavity.

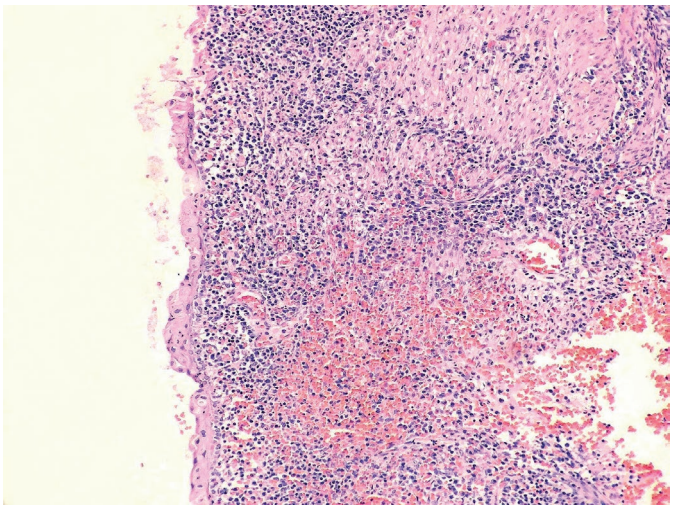

Fig. 5 Detail on massive inflammation of the atrophic endometrium and adjacent myometrium (hematoxylin & eozin, ×100).

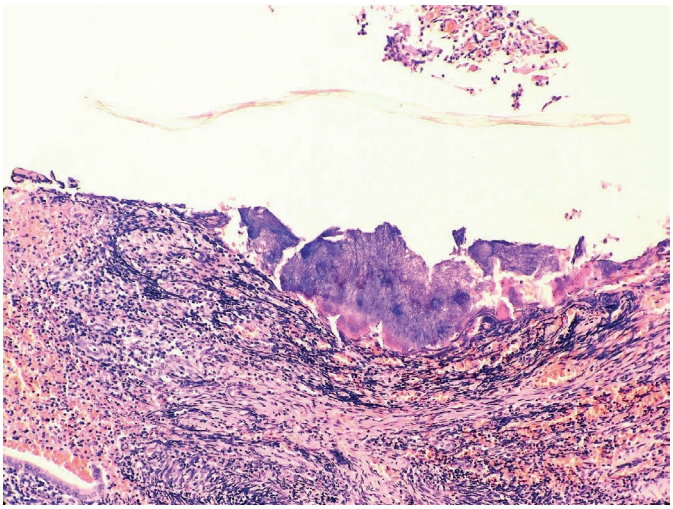

Fig. 6 Chronic active endomyometritis with Actinomyces colonies in the centre (hematoxylin & eozin, ×40).

DISCUSSION

At the present time, actinomycosis of the uterus is an extremely rare disease. In a recent study, Chiesa-Vottero (3) has found only seven cases (0.02%) of actinomycotic endometritis among 28,906 endometrial biopsies. Actinomycosis of the female genital tract is directly related to long-term use of the IUDs, especially for more than 5 years (1, 2). Prolonged insertion of an IUD causes mild inflammatory changes in the endometrium with necrosis that creates an anaerobic environment that favors the growth of the Actinomycetes (2). Although this association

Tab. 1 Summary of the clinical findings of the patients extracted from the published case reports.

Ref.	Patient age	IUD use	Clinical manifestation
[2]	76 years	44 years	vaginal bleeding, pelvic pain, mild febrility
[6]	58 years	33 years	vaginal bleeding and spotting
[7]	67 years	35 years	acute abdominal pain, perforation of the uterus
[8]	55 years	27 years	vaginal bleeding and spotting
[9]	59 years	22 years	blood-stained vaginal discharge, mild febrility
this case	70 years	42 years	blood-stained vaginal discharge

is generally well-known, it is not possible to quantify an actual risk of disease. Approximately 7–13.7% of women using an IUD may have a finding of Actinomyces-like microorganisms on a Papanicolaou test (4, 5). However, the prognostic significance of this finding is minimal because the vast majority of them will remain without any signs of disease (4, 5). For example, in the study of Kalaichelvan et al. (5), 150 out of 152 IUD users (98.7%) with Actinomyces-positive cervical smears were asymptomatic, while only two (1.3%) developed a pelvic inflammatory disease at 6 months. Therefore, in the absence of clinical symptoms, women with Actinomyces-like organisms on a Papanicolaou test do not need preemptive antibiotic treatment, even do not require IUD removal (4, 5). However, because one can not predict which IUD user colonized by Actinomyces will develop severe pelvic infection, all of them should have a periodical gynecological follow-up.

In the current paper, we have presented a rare case of postmenopausal woman with an actinomycotic endomyometritis associated with a long-term use of an IUD lasting for 42 years. To our knowledge, only a few articles desribing an endometrial actinomycosis related to such a long interval of an IUD insertion has been published until now. We have reviewed five such cases, which are briefly summarized in Table 1 (references 2, 6–9) including our present case. All females were postmenopausal with the mean age of 63 years. The time of an IUD insertion ranged from 22 to 44 years. The main clinical symptoms were vaginal discharge and bleeding. A very uncommon case has been published by Phupong et al. (7), who reported a 67-year-old woman manifesting with an acute abdominal pain due to spontaneous perforation of the uterus from actinomycotic infection with Lippes loop IUD.

In conclusion, wearing an IUD continuously for very long periods of time can lead to actinomycotic infection, which may manifest for many years after its application. As this method of contraception is being used much less frequently than in the past, such cases as we have described become a rarity. Anyway, all IUD users have to keep in mind regular gynecological check-ups to avoid the complications of a retained and "forgotten" IUD.

ACKNOWLEDGEMENTS

The authors would like to thank all physicians from Faculty Hospital in *Žilina,* who participated on treatment and clinical management of the patient.

REFERENCES

1. Heo SH, Shin SS, Kim JW, et al. Imaging of actinomycosis in various organs: a comprehensive review. Radiographics 2014; 34: 19–33.
2. Prabhala S, Erukkambattu J, Basavanapalli M, Tanikella R. Endometrial actinomycosis associated with intrauterine contraceptive device forgotten for 44 years. Med J DY Patil Univ 2016; 9: 231–3.
3. Chiesa-Vottero AG. Actinomycotic endometritis. Int J Gynecol Pathol 2019; 38(2): 138–42.
4. Westhoff C. IUDs and colonization or infection with Actinomyces. Contraception 2007; 75(6 Suppl): S48–50.
5. Kalaichelvan V, Maw AA, Singh K. Actinomyces in cervical smears of women using the intrauterine device in Singapore. Contraception 2006; 73: 352–5.
6. Sozen I, Morgan K, Shannon JS. Postmenopausal bleeding secondary to a Dalkon Shield retained for 33 years: a case report. J Reprod Med 2005; 50: 216–8.
7. Phupong V, Sueblinvong T, Pruksananonda K, Taneepanichskul S, Triratanachat S. Uterine perforation with Lippes loop intrauterine device-associated actinomycosis: a case report and review of the literature. Contraception 2000; 61: 347–50.
8. Shweta N, Nandini JU, Laxmi PV. Pelvic actinomycosis associated with long term use of intrauterine contraceptive device. J Obstet Gynecol India 2010; 60: 345–7.
9. Kriplani A, Buckshee K, Relan S, Kapila K. "Forgotten" intrauterine device leading to actinomycotic pyometra 13 years after menopause. Eur J Obstet Gynecol Reprod Biol 1994; 53: 215–6.

Intradural Extramedullary Epidermoid Cyst at the Conus Medullaris level with Thoracic Syringomyelia: a Case Report

Bekir Akgun[1,*], Ahmet Cemil Ergun[1], Ibrahim Hanifi Ozercan[2], Selman Kok[1]

ABSTRACT

Spinal epidermoid cysts are benign tumors. Syringomyelia secondary to intramedullary tumors are frequently observed. However, the association between syringomyelia and spinal intradural extramedullary epidermoid cyst in the conus medullaris region is extremely rare. We present the case of a 3-year-old male who was admitted with paraparesis and urinary retention. Magnetic resonance imaging (MRI) of the spine demonstrated intradural extramedullary lesion, compatible with epidermoid cyst, that at the conus medullaris level and a large syringomyelia extending from T4 to L1 vertebrae. Total microsurgical excision of the cyst was performed. No additional drainage was carried out for the syringomyelic cavity. Histopathological examination verified the diagnosis of the epidermoid cyst. Total excision of the cyst and disappearance of the syringomyelia were observed on MRI at 15 days postoperatively. We have clarified the etiology, clinical, histopathological and radiological features, differential diagnosis, and treatment modalities of spinal epidermoid cysts. In addition, we have discussed the possible mechanisms of syringomyelia formation in spinal intradural lesions.

KEYWORDS

conus medullaris; epidermoid cyst; syringomyelia; spine

AUTHOR AFFILIATIONS

[1] Firat University Hospital, Departments of Neurosurgery Elazig, Turkey
[2] Firat University Hospital, Clinical Pathology, Elazig, Turkey
* Corresponding author: Firat Universitesi Hastanesi, Beyin Cerrahisi Klinigi, 23119, Elazig, Turkey; e-mail: bekirakgun@yahoo.com

Received: 12 July 2018
Accepted: 10 November 2018
Published online: 1 April 2019

Acta Medica (Hradec Králové) 2019; 62(1): 39–42
https://doi.org/10.14712/18059694.2019.45

INTRODUCTION

The term "inclusion cysts" includes dermoid and epidermoid tumors/cysts. They are derived from cutaneous ectoderm (1). Spinal epidermoid cysts are rare and slow-growing benign lesions. They constitute <1% of all spinal tumors (2, 3). Most of the spinal epidermoid cysts are located in the lumbosacral and thoracic regions (4). Conus medullaris epidermoid cysts are extremely rare entities.

Syringomyelia is characterized by the presence of cystic cavities inside the spinal cord. It is a secondary process with many etiologies. Chiari malformations, neoplasms, arteriovenous malformations, arachnoiditis, and spinal dysraphisms are some examples (5). Syringomyelia associated with intramedullary tumors are frequently observed. The most common tumors associated with syringomyelia are astrocytomas and ependymomas. In addition, their most common locations are the lower cervical and upper thoracic regions (6, 7). However, extramedullary tumors at the conus medullaris level associated with syringomyelia are uncommon coexistences. Here we describe and discuss the case of a patient with conus medullaris epidermoid cyst associated with a large thoracic syringomyelia.

CASE REPORT

A 3-year-old male was admitted with increasingly leg weakness that had persisted for 2 months. Neurologic examination revealed that the proximal and distal muscular forces in his right and left lower extremities were 3/5 and 2/5, respectively. A large syringomyelia, extending from T4 to L1 vertebrae, was detected on thoracic magnetic resonance imaging (MRI). In lumbar MRI, T1-weighted imaging demonstrated isointense expansion at the L1-2 vertebrae level. T2-weighted imaging revealed an intradural extramedullary regular lesion that had hyperintense capsule-like formation with isointense content and that excessively compressed the conus medullaris. It was approximately 15 × 15 mm in size. T1-gadolinium-enhanced imaging showed that dense cystic mass had circumferential contrast enhancement. Besides, some cauda equina fibers had contrast enhancement (Figure 1). In addition, renal ultrasonography was performed before and after micturition. Significant post-micturition residue was determined. He underwent surgery. Total microsurgical excision of the lesion was achieved with the help of neuromonitoring after L1 and L2 laminotomies. Also, the integrity of the facet joints was protected. After dural opening, the lower end of the spinal cord (conus medullaris) and the beginning of the cauda equina fibers appeared compressed by an anterior extramedullary lesion. Dense pearly content and whitish cyst capsule were completely excised. No additional drainage procedure for the syringomyelic cavity was considered at this surgical intervention. Besides, CSF leakage was not observed from the neighbouring syringomyelic cavity after cyst removal. In the closure, L1 and L2 laminoplasties were performed. In the early postoperative period, muscular force in his right and left lower extremities had improved to 4/5 and 3/5, respectively. Histological examination of the specimens demonstrated that the cyst walls were lined with stratified squamous epithelium without skin adnexa. Furthermore, desquamation of keratin from the epithelial lining was detected. This examination revealed epidermoid cyst (Figure 2). There was no finding of residual tumor on MRI at 15 days postoperatively. In addition, disappearance of the syringomyelia was seen. However hyperintensity at T2 weighted image compatible with myelomalacia, existed after the cyst resection, was observed (Figure 3A,B,C). At 20 days postoperatively, renal ultrasonography was performed before and after micturition, which showed decreased post-micturition residue. Physical therapy and rehabilitation were indicated at 1 month postoperatively. In the second month control his examination revealed no neurological deficits. Besides, significant decrease of myelomalacia was seen at the second month follow-up MRI. (Figure 3D).

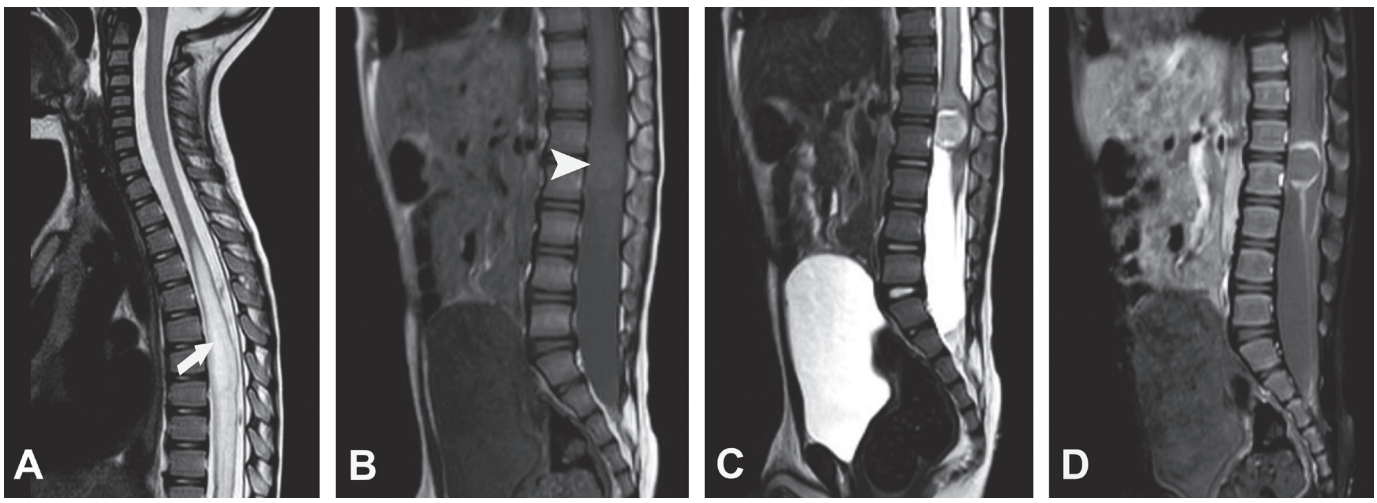

Fig. 1 In the preoperative (A) thoracic MRI, a syringohydromyelia (arrow), extending from T4 to L1 vertebrae, was observed. Lumbar MRI (B) T1-weighted sagittal image showed hypointense expansion (arrowhead) at the L1-2 vertebrae level. (C) T2-weighted image showed a lesion that had hyperintense capsular formation with isointense content and that excessively compressed the conus medullaris. (D) T1-gadolinum-enhanced image demonstrated that dense cystic mass had circumferential contrast enhancement. Besides, some cauda equina fibers had contrast enhancement.

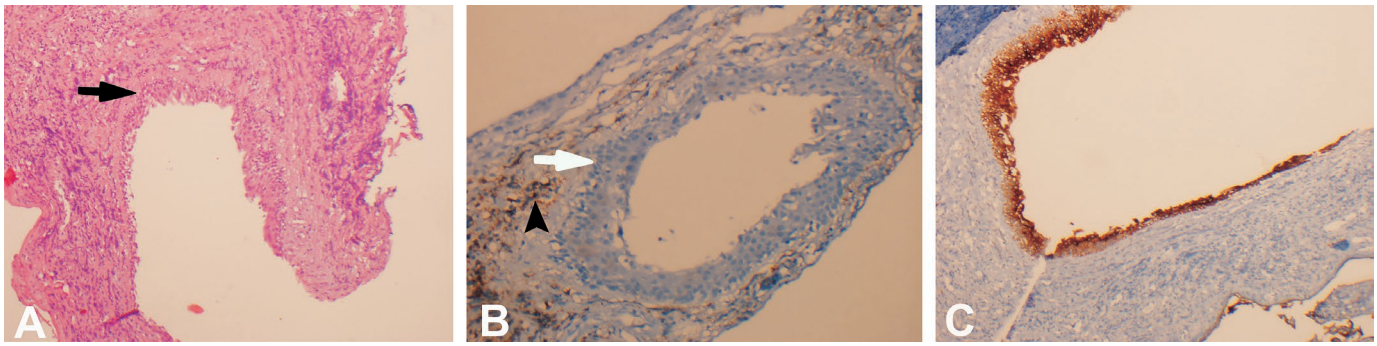

Fig. 2 In the histopathological examination, (A) cystic lesion with stratified squamous epithelium (black arrow) (hematoxylin–eosin, ×100). (B) Inflammatory cells (arrowhead), stained by leukocyte common antigen (LCA), around the cystic lesion with stratified squamous epithelium (white arrow) (LCA, ×100). (C) Stratified squamous epithelium stained with pancytokeratin. Desquamation of keratin from the epithelial lining can be observed (pancytokeratin, ×100).

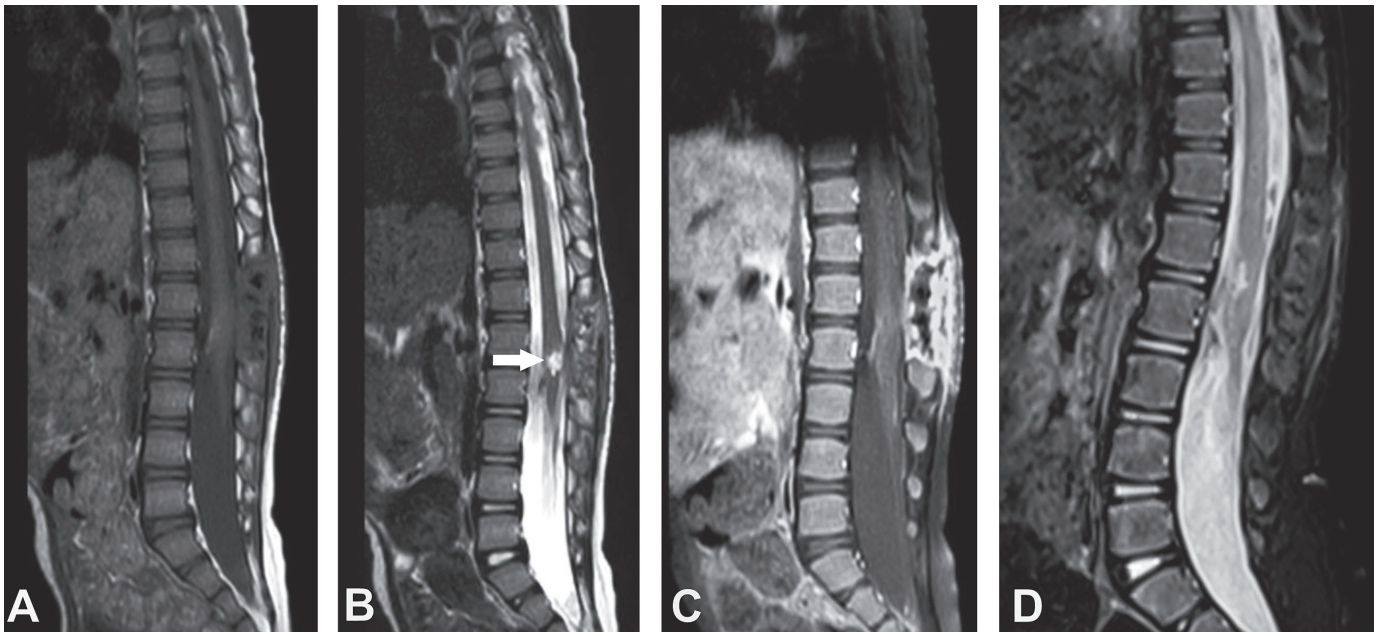

Fig. 3 Postoperative MRIs. Disappearance of the syringohydromyelia was observed. There was no finding of residual tumor. Decompression of the conus medullaris and cauda equina fibers is shown. (A) T1-weighted, (B) T2-weighted (arrow: hyperintense image thought to be myelomalacia due to chronic compression, which existed after the cyst resection), and (C) contrasted sagittal section at 15 days postoperatively. (D) T2-weighted sagittal section also showed significant decrease of myelomalacic aspect at 60 days postoperatively.

DISCUSSION

Spinal epidermoid cysts may be acquired or congenital. Acquired epidermoid cysts, due to iatrogenic penetration of skin fragments, have been frequently reported after lumbar puncture or meningomyelocele repair with years of latency (1, 8, 9). Congenital spinal epidermoid cyst is thought to be an inclusion of ectodermal tissues during closure of the neural tube between the third and fourth weeks of embryonic development (3). Occult spinal dysraphisms, spina bifida aperta, hemivertebra, and dermoid tracts are often associated with congenital cysts (1, 3, 8). Our patient had no known history of meningomyelocele repair such as open wound trauma or lumbar puncture; therefore, the tumor was thought to be congenital.

Signs and symptoms arising from epidermoid cysts vary with the extent of involvement and are not different from other spinal space-occupying lesions. Paraparesis, sensory loss, urological manifestations, pathologic reflex appearance, deep tendon reflex changes, and back/extremity pain are usually found at presentation. The slow growth of epidermoid cysts often leads to a delay in their diagnosis (2).

MRI is useful for diagnosis, particularly contrast-enhanced studies, which also show the exact location and extension of the lesion. MRI demonstrates that epidermoid cyst is hypointense on T1-weighted and hyperintense on T2-weighted images (8). Peripheral postgadolinium enhancement with well-defined limits without perilesional edema contributes to diagnosis. Some authors emphasize that peripheral enhancement represents normal peripheral surrounding tissue reaction, whereas others consider it as an outer capsule composed of tumor cells (9). In this patient, circumferential contrast enhancement was due to capsular formation. However, contrast enhancement of the some cauda equina fibers might be reactional. During

the operation, we observed conspicuous capsular formation; therefore, we obtained tissue samples as well as the capsule-like formation and dense content of the cyst for histopathological examination.

Ependymomas are the most common space-occupying lesions at the conus medullaris–cauda equina level. Lymphomas, astrocytomas, gangliogliomas, and ganglioneuromas can be considered during differential diagnosis (7, 10, 11). They can be frequently identified and distinguished by MRI studies. Astrocytomas, gangliogliomas, and ganglioneuromas have heterogeneous contrast patterns. Ependymomas have homogenous contrast enhancement, and epidermoid cysts have peripheral contrast enhancement (7, 9, 11). Nevertheless, radiological differentiation is sometimes difficult for these spinal lesions, but they can be histopathologically diagnosed.

Histopathological examination is critical for diagnosing of epidermoid cysts. Differentiation between the two forms of inclusion tumors (dermoid/epidermoid) is based on the presence of adnexal skin structures, such as sebaceous glands, eccrine glands, and hair follicles. They are present only in dermoid cysts (1, 2). A specific histological feature of the epidermoid cyst is a lined stratified squamous keratinizing epithelium surrounded by an outer layer of collagenous tissue and/or inflammatory cells without skin adnexa. Desquamation of keratin from the epithelial lining generates cholesterol crystals (2, 9).

Total excision including the capsule is the curative treatment for spinal epidermoid cyst because it is a benign condition. Sometimes, because of its anatomical features, intramedullary tumor shows tight adherence to the arachnoid membrane and spinal cord, thereby causing some surgical difficulties for safe and complete resection. Therefore, subtotal resection is also commonly performed to avoid neurological deficits (1, 2). Local recurrence is reported especially after subtotal excision. Incomplete excision of basal germinal cells of the tumor is suggested to be the cause of recurrence (12). Long-term follow-up is necessary for tumor recurrence risk. Surgeons should keep in mind that cyst content includes fat and cholesterol. These can cause an inflammatory reaction that leads to aseptic chemical meningitis (Mollaret's meningitis) (8). Plugging of proximal and distal arachnoid spaces and irrigating the site with normal saline prior to dural closure reduces the risk of chemical meningitis (9). We performed total excision in this case. Besides, the patient did not develop any inflammatory reactions and neurological deterioration postoperatively.

The exact pathogenesis of syringomyelia accompanied with spinal cord tumors is unclear. Different theories have been proposed. Some of them are intramedullary softening due to an impaired blood circulation, stasis of tissue fluid resulting from occlusion of the drainage pathways, effect of edema, and spontaneous autolytic reactions of the tumor (7, 13). Another suggested mechanism of syrinx formation was obstruction of cerebrospinal fluid (CSF) flow (13, 10, 14). Given these possible reasons, syringomyelia associated with intramedullary tumors can be frequently observed. However, extramedullary tumors associated with syringomyelia are very rare. In our case, syringomyelia most likely developed secondary to the mass effect of the epidermoid cyst. It has been postulated that cyst may cause blockage of CSF flow dynamics. Accordingly, excision of the cyst can remove the mass effect and regenerate these CSF flow alterations. Hence, after the total resection of the cyst, disappearance/reduction of the syrinx cavity was achieved, in spite of CSF leakage was not observed from the neighbouring syringomyelic cavity. Besides, no additional drainage procedure for the syringomyelic cavity was considered.

In conclusion, spinal intradural extramedullary epidermoid cyst at the conus medullaris level associated with thoracic syringomyelia is a very rare entity. MRI is very useful for diagnosis, identifying the exact location of the cyst, and detecting comorbidities. The clinical course is dependent on the neurological condition of the patient at presentation and any delay in the diagnosis. Moreover, appropriate early surgical intervention with total excision results in good prognosis. Syringomyelia most likely developed secondary to the mass effect of the cyst and blockage of the CSF flow dynamics. Therefore, excision of the cyst can ensure the disappearance or reduction of the syringomyelia.

REFERENCES

1. Thompson DNP. Spinal inclusion cysts. Childs Nerv Syst 2013; 29: 1647–55.
2. Gotecha S, Ranade D, Sharma S, Punia P, Kotecha M. Giant intradural intramedullary epidermoid cyst Report of two cases with varied presentations. Asian J Neurosurg 2014; 9: 244.
3. Manno NJ, Uihlein A, Kernohan JW. Intraspinal epidermoids. J Neurosurg 1962; 19: 754–65.
4. Ferrara P, Costa S, Rigante D, et al. Intramedullary epidermoid cyst presenting with abnormal urological manifestations. Spinal Cord 2003; 41: 645–8.
5. Su DK, Ebenezer S, Avellino AM. Symptomatic Spinal Cord Compression from an Intradural Arachnoid Cyst with Associated Syrinx in a Child: Case Report. Pediatr Neurosurg 2012; 48: 236–9.
6. Quencer RM, el Gammal T, Cohen G. Syringomyelia associated with intradural extramedullary masses of the spinal canal. AJNR Am J Neuroradiol 1986; 7: 143–8.
7. Sarikaya S, Acikgoz B, Tekkok IH, Gungen YY. Conus ependymoma with holocord syringohydromyelia and syringobulbia. Journal of Clinical Neuroscience 2007; 14: 901–4.
8. Funao H, Isogai N, Daimon K, et al. A rare case of intradural and extramedullary epidermoid cyst after repetitive epidural anesthesia: case report and review of the literature. World Journal of Surgical Oncology 2017; 15: 131.
9. Mishra SS, Satapathy MC, Deo RC, Tripathy SR, Senapati SB. Isolated thoracic (D5) intramedullary epidermoid cyst without spinal dysraphism: A rare case report. J Pediatr Neurosci 2015; 10: 133–6.
10. Nagahiro S, Matsukado Y, Kuratsu J, Saito Y, Takamura S. Syringomyelia and syringobulbia associated with an ependymoma of the cauda equina involving the conus medullaris: case report. Neurosurgery 1986; 18: 357–60.
11. Wang K, Dai J. Conus medullaris ganglioneuroma with syringomyelia radiologically mimicking ependymoma: A case report. Oncology Letters 2015; 10: 3803–6.
12. Penisson-Besnier I, Guy G, Gandon Y. Intramedullary epidermoid cyst evaluated by computed tomographic scan and magnetic resonance imaging: case report. Neurosurgery 1989; 25: 955–9.
13. Samii M, Klekamp J. Surgical results of 100 intramedullary tumors in relation to accompanying syringomyelia. Neurosurgery 1994; 35: 865–73.
14. Blaylock RL. Hydrosyringomyelia of the conus medullaris associated with a thoracic meningioma: case report. J Neurosurg 1981; 54: 833–5.

REVIEWER, THANK YOU

The editors greatly appreciate the support of all reviewers whose comments and scientific evaluation of submitted manuscripts are invaluable for ensuring the scientific quality of this journal. The following distinguished clinicians and scientists acted as reviewers:

Pavel Babál, Bratislava, Slovakia
Marek Ballon, Hradec Králové, Czech Republic
Jiří Beran, Prague, Czech Republic
Alex Blackwell, Worcester, United Kingdom
Vladimír Blaha, Hradec Králové, Czech Republic
Petr Broulík, Prague, Czech Republic
Miroslav Brozman, Nitra, Slovakia
Radan Brůha, Prague, Czech Republic
Xun-Zi Cai's, Hangzhou, China
Helena Čermáková, Hradec Králové, Czech Republic
Pavlína Černochová, Brno, Czech Republic
Viktor Chrobok, Hradec Králové, Czech Republic
Lucia Cugusi, Monserrato, Italy
Srijit Das, Kuala Lumpur, Malaysia
Milan Dastych, Brno, Czech Republic
Ivo Dřížhal, Hradec Králové, Czech Republic
Stanislav Filip, Hradec Králové, Czech Republic
Martin Frank, Hradec Králové, Czech Republic
Roman Fraško, Prague, Czech Republic
Zdeněk Fryšák, Olomouc, Czech Republic
Filip Gabalec, Hradec Králové, Czech Republic
Sylva Gilbertová, Prague, Czech Republic
Igor Guňka, Hradec Králové, Czech Republic
Robert Gürlich, Prague, Czech Republic
Lenka Hobzová, Hradec Králové, Czech Republic
Pavel Horák, Olomouc, Czech Republic
Tomáš Hosszú, Hradec Králové, Czech Republic
Anna Hošťálková, Hradec Králové, Czech Republic
Dana Jurkovičová, Bratislava, Slovakia
Michal Jurovčík, Prague, Czech Republic
Marian Kacerovský, Hradec Králové, Czech Republic
Milan Kaška, Hradec Králové, Czech Republic
Jan Kilian, Pilsen, Czech Republic
Romana Koberová Ivančaková, Hradec Králové, Czech Republic
Vladimír Koblížek, Hradec Králové, Czech Republic
Ján Kočiš, Brno, Czech Republic
Zdeněk Kokštein, Hradec Králové, Czech Republic
Marcela Kopáčová, Hradec Králové, Czech Republic
Jaroslav Koudelka, Hradec Králové, Czech Republic
Jan Kovář, Prague, Czech Republic
Zahari Krastev, Sofia, Bulgaria
Irena Krčmová, Hradec Králové, Czech Republic
Hana Krejčí, Prague, Czech Republic
Stanislav Malý, Prague, Czech Republic
Alexander Mamourian, Philadelphia, USA
Antony McNamee, Brisbane, Australia
Bohuslav Melichar, Olomouc, Czech Republic
Zdeněk Merta, Brno, Czech Republic
Stanislav Mičuda, Hradec Králové, Czech Republic
Ivana Musilová Kacerovská, Hradec Králové, Czech Republic
Shoeb Mustafa, Riyadh, Kingdom of Saudi Arabia
Sherine Adel Nasry, Cairo, Egypt
David Neumann, Hradec Králové, Czech Republic
Hadži D. Nikolov, Kolín, Czech Republic
Július Örhalmi, Hradec Králové, Czech Republic
George Pados, Thessaloniki, Greece
Vladimír Palička, Hradec Králové, Czech Republic
Charalampos Papagoras, Alexandroupolis, Greece
Jiří Petera, Hradec Králové, Czech Republic
Jan Piťha, Hradec Králové, Czech Republic
Miroslav Podhola, Hradec Králové, Czech Republic
Jiří Presl, Pilsen, Czech Republic
Jakub Radocha, Hradec Králové, Czech Republic
Olga Rejtarová, Hradec Králové, Czech Republic
Ioannis Rouvelas, Stockholm, Sweden
Pavel Rozsíval, Hradec Králové, Czech Republic
Rolf de Ruijter, Groningen, Netherlands
Elnaz Sadeghi, Albuquerque, New Mexico, USA
Richard Salzman, Olomouc, Czech Republic
Jitka Schreiberová, Hradec Králové, Czech Republic
Iva Sedláková, Hradec Králové, Czech Republic
David Školoudík, Olomouc, Czech Republic
Tomáš Soukup, Rheumatology, Hradec Králové, Czech Republic
Tomáš Soukup, Histology, Hradec Králové, Czech Republic
Milan Sova, Olomouc, Czech Republic
Jiří Špaček, Hradec Králové, Czech Republic
Miloš Špidlen, Olomouc, Czech Republic
Pavel Šponer, Hradec Králové, Czech Republic
Zbyněk Straňák, Prague, Czech Republic
Zdeněk Šubrt, Hradec Králové, Czech Republic
Ilja Tachecí, Hradec Králové, Czech Republic
Vladimír Třeška, Pilsen, Czech Republic
Kamran Urgun, Irvine, USA
Ivan Vařeka, Hradec Králové, Czech Republic
Petr Vlček, Prague, Czech Republic
Jan Vodička, Pardubice, Czech Republic
Hiroshi Yokomichi, Chuo City, Yamanashi, Japan
Fani Zacharaki, Larissa, Greece
Karel Zadrobílek, Hradec Králové, Czech Republic

The Editors hereby express their sincere gratitude for and their appreciation of the work done as well as the support given to this journal.